RESEARCH

Vincamine as a GPR40 agonist improves glucose homeostasis in type 2 diabetic mice

Te Du[1,2], Liu Yang[1,2], Xu Xu[3], Xiaofan Shi[1,2], Xin Xu[1,2], Jian Lu[3], Jianlu Lv[3], Xi Huang[3], Jing Chen[1,2], Heyao Wang[1,2], Jiming Ye[4], Lihong Hu[3] and **Xu Shen[1,2,3]**

[1]Shanghai Institute of Materia Medica, Chinese Academy of Sciences, Shanghai, China
[2]School of Pharmacy, University of Chinese Academy of Sciences, Beijing, China
[3]School of Medicine and Life Sciences, Nanjing University of Chinese Medicine, Nanjing, China
[4]School of Health and Biomedical Sciences, RMIT University, Victoria, Australia

Correspondence should be addressed to J Chen or L Hu or X Shen: jingchen@simm.ac.cn or lhhu@njucm.edu.cn or xshen88@163.com

Abstract

Vincamine, a monoterpenoid indole alkaloid extracted from the Madagascar periwinkle, is clinically used for the treatment of cardio-cerebrovascular diseases, while also treated as a dietary supplement with nootropic function. Given the neuronal protection of vincamine and the potency of β-cell amelioration in treating type 2 diabetes mellitus (T2DM), we investigated the potential of vincamine in protecting β-cells and ameliorating glucose homeostasis *in vitro* and *in vivo*. Interestingly, we found that vincamine could protect INS-832/13 cells function by regulating G-protein-coupled receptor 40 (GPR40)/cAMP/Ca^{2+}/IRS2/PI3K/Akt signaling pathway, while increasing glucose-stimulated insulin secretion (GSIS) by modulating GPR40/cAMP/Ca^{2+}/CaMKII pathway, which reveals a novel mechanism underlying GPR40-mediated cell protection and GSIS in INS-832/13 cells. Moreover, administration of vincamine effectively ameliorated glucose homeostasis in either HFD/STZ or *db/db* type 2 diabetic mice. To our knowledge, our current work might be the first report on vincamine targeting GPR40 and its potential in the treatment of T2DM.

Key Words

- vincamine
- GPR40
- β-cell function
- insulin secretion
- type 2 diabetes

Journal of Endocrinology (2019) **240**, 195–214

Introduction

Type 2 diabetes mellitus (T2DM) is a severe worldwide disease, mainly characterized by insulin resistance and dysfunction of pancreatic β-cells (Olokoba *et al.* 2012). Within insulin resistance, β-cells increase insulin release to maintain normal glucose tolerance (Spellman 2007). When β-cells fail to compensate for the decreased insulin sensitivity, T2DM may occur, resulting in hyperglycemia, deterioration of β-cells, chronic health problems and even death (Prentki & Nolan 2006). As such, β-cell dysfunction is one of the key contributors to T2DM.

Pathologically, pancreatic β-cell dysfunction involves a combination of decreased β-cell mass and impaired insulin secretion (Prentki & Nolan 2006). The mass of β-cells is mainly regulated by apoptosis, size modification, replication and neogenesis, while β-cell apoptosis determines the onset and rate of T2DM progression (Bonner-Weir 2000). It was reported that a series of genetic alterations including G protein-coupled receptors, Akt, IRS2, PTEN, Fas/FasL, NF-κb, Bcl2 family, caspase family, ion channels and so on are tightly associated with β-cell apoptosis (Anuradha *et al.* 2014, Reimann & Gribble 2016), and some of the β-cell apoptosis-related proteins have been proved as potential targets for anti-T2DM drug discovery, further illustrating the importance of β-cell apoptosis in T2DM.

Clinically, several anti-diabetic drugs have been used for improving β-cell dysfunction, such as sulfonylurea

https://joe.bioscientifica.com
https://doi.org/10.1530/JOE-18-0432

derivatives (SUs), DPP4 inhibitors and incretin hormone GLP-1 analogs, although none of them has been successful in controlling long-term microvascular and macrovascular complications (Zarich 2009). To improve curative effects, many medicinal herbs and their extracts have also been applied in the treatment of diabetes, and discovery of efficient β-cell protectors from natural resources has attracted much attention, while lots of active compounds have been determined, including curcumin, gymnema sylvestre, berberine and *Vinca rosea* (Hosseini *et al*. 2015).

Vincamine (Fig. 1A) is a monoterpenoid indole alkaloid found in the Madagascar periwinkle (Fandy *et al*. 2016). It increases cerebral blood flow, oxygen consumption and glucose utilization and improves dementia and memory disturbance (Hagstadius *et al*. 1984). Vincamine is commercially available in the United States as a health care product with nootropic function (Fandy *et al*. 2016). Recently, common features between β-cells and neurons have been widely investigated. For example, some neurotransmitters have been determined to modulate insulin and glucagon secretion, and the components of neuronal signaling systems are expressed in islets (Rodriguez-Diaz *et al*. 2012, Otters & Lammert 2016). Similar to the pathology of T2DM, the impairment of neuronal insulin receptor (IR) also leads to insulin resistance (Li *et al*. 2015). Moreover, agents with neuronal protection may exhibit potential in islet amelioration. For example, dextromethorphan can improve neuron degeneration and protect β-cells (Marquard *et al*. 2015, Xu *et al*. 2016). Therefore, we wondered whether vincamine might have a similar effect on endocrine cells as it does on neural cells, and it might also exhibit hypoglycemic property in treating T2DM.

In the current work, we discovered that vincamine functioned as GPR40 agonist to effectively protect INS-832/13 cells by regulating GPR40/cAMP/Ca^{2+}/IRS2/PI3K/Akt signaling pathway and stimulating GSIS by modulating GPR40/cAMP/Ca^{2+}/CaMKII pathway. Assays in HFD/STZ and *db/db* mice have further verified the benefit of vincamine in ameliorating glucose homeostasis. Taken together, our results have highlighted the possibility of vincamine in the treatment of T2DM.

Materials and methods

Materials

H89 and wortmannin were from Selleck. Puromycin was from YEASAN (Shanghai, China) and GW1100 was from MedChem Express (Monmouth Junction, NJ, USA). All other reagents were from Sigma-Aldrich. Antibody against Phospho-FOXO1 (Ser256) and antibodies against IRS2 for immunofluorescence (IF) were from Abcam, GPR40 was from Novus (Littleton, CO, USA) and GAPDH was from Kangcheng Biotech (Shanghai, China). Antibodies against insulin and cleaved Caspase 3 for IF were from Servicebio Technology Company (Wuhan, China). The rest of the antibodies were from Cell Signaling Technology. Cell culture medium and supplements were from Invitrogen.

Cell culture

INS-832/13 cells

INS-832/13 cells were cultured in RPMI-1640 medium supplemented with 10% FBS (Gibco), 100 U/mL penicillin and 100 mg/mL streptomycin, 2 mM L-glutamine, 1 mM sodium-pyruvate, 0.05 mM β-mercaptoethanol and 10 mM HEPES.

hGPR40-CHO cells

CHO cells were stably transfected to express human-GPR40 and maintained in F12 medium containing 10% FBS, 100 U/mL penicillin, 100 mg/mL streptomycin and 500 μg/mL G418.

INS-832/13 and CHO cells were purchased from ATCC, passage numbers of the cell lines used for the experiments were 3–15th.

Mouse primary hepatocyte isolation

Isolation of mouse primary hepatocytes was performed according to the published approach (Mathijs *et al*. 2009). Briefly, the liver was perfused with 0.5 mM EGTA-containing PBS buffer (137 mM NaCl, 2.7 mM KCl, 10 mM Na_2HPO_4, 2 mM KH_2PO_4, pH 7.3) for 5 min, and then replaced with DMEM medium supplemented with collagenase (0.5 mg/mL) for 5–10 min. Then, cells were released into iced standard Williams' E medium (containing 10% FBS, 100 U/mL penicillin and 100 mg/mL streptomycin), followed by filtration with a sterile 70-μm mesh nylon filter. After centrifugation (50***g***, 5 min, 4°C), cells were re-suspended by standard Williams' E medium with 50% Percoll solution (GE Healthcare) and centrifuged (1000***g***, 10 min, 4°C) again to harvest fresh hepatocytes.

Cell viability assay

MTT assay

INS-832/13 cells were seeded into 96-well plates (4×10^4 cells/well). After overnight culture, cells were treated

https://joe.bioscientifica.com
https://doi.org/10.1530/JOE-18-0432

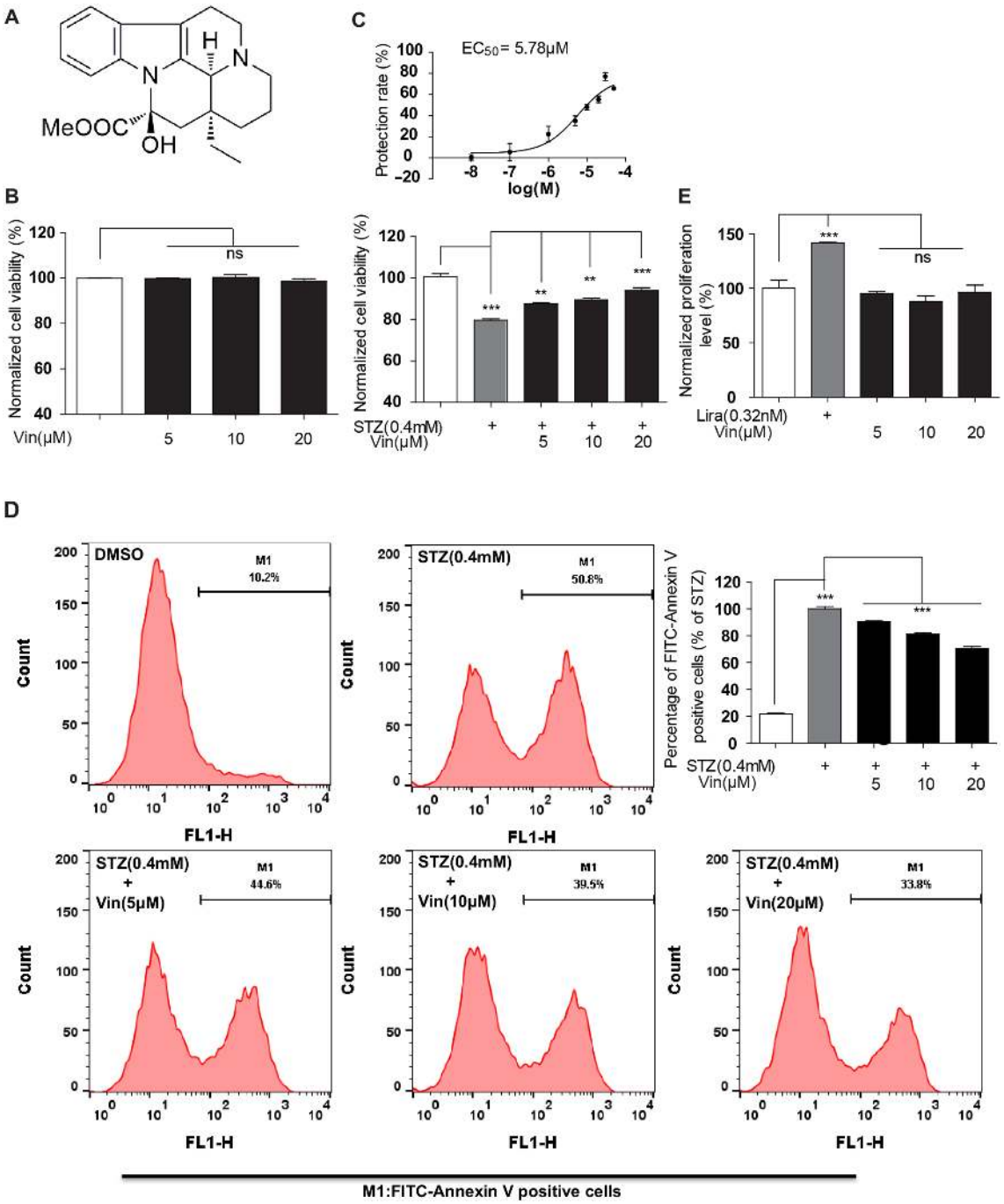

Figure 1

Vincamine promotes β-cell survival. (A) Chemical structure of vincamine. (B) In the absence of STZ, INS-832/13 cells were incubated with vincamine (5, 10, 20 μM) for 24 h, and then MTT assay was applied. (C) MTT assay was performed after incubation with STZ (0.4 mM) and vincamine (5, 10, 20 μM) in INS-832/13 cells for 24 h. EC_{50} of vincamine was fitted by GraphPad Prism. (D) INS-832/13 cells treated as C were stained with Annexin V-FITC, followed by the determination of flow cytometry. (E) CyQUANT GR dye was used to detect 480/520 nm fluorescence in INS-832/13 cells treated with Liraglutide (0.32 nM) or vincamine (5, 10, 20 μM) for 24 h. Data were shown as means ± S.E.M. with three independent experimental replicates. Significant differences between groups are represented as $^{**}P < 0.01$ and $^{***}P < 0.001$, and $P > 0.05$ stood for no significance (ns). (Vin, as vincamine.)

https://joe.bioscientifica.com
https://doi.org/10.1530/JOE-18-0432

with test compounds and STZ (0.4 mM) for 24 h and then incubated with 0.5 mg/mL MTT for 4 h to form formazan crystals. Finally, these crystals were dissolved in DMSO, and the absorbance was determined at 570 nm.

Proliferation assay

Proliferation assay was conducted in INS-832/13 cells treated with corresponding compounds according to a protocol of CyQUANT Cell Proliferation Assay Kit (Invitrogen, Molecular Probes).

Flow cytometry analysis

INS-832/13 cells were plated into 12-well plates (1×10^6 cells/well) and allowed to grow overnight, and then cells were treated with corresponding compounds. The collection and treatment of cells were carried out using FITC Annexin V Apoptosis Detection Kit I (BD, San Jose, CA, USA) according to the manufacturer's protocol. The number of apoptotic cells was quantified by BD FACS Calibur flow cytometer. Each sample required 10,000 events for detection.

p-Akt (Ser 473) AlphaLISA assay

INS-832/13 cells were grown in 96-well plates (5×10^4 cells/well) and allowed to attach overnight. Then, cells were incubated with corresponding compounds for 24 h. Cells lysates were collected to examine p-Akt (Ser473) content by using AlphaLISA SureFire Ultra p-Akt (Ser473) Assay Kits (PerkinElmer).

RNA isolation and quantitative real-time PCR

INS-832/13 cells were plated into 6-well plates (9×10^5 cells/well) with overnight culture. The cells were incubated with corresponding compounds for 24 h and washed in PBS, and then total mRNA in cells were gathered using RNAiso Plus (TakaRa). Synthesis of first-strand cDNA was performed using PrimeScript RT Master Mix (TaKaRa). The quantity of mRNA was detected by quantitative real-time PCR (qRT-PCR) using the SYBR Premix Ex Taq (TaKaRa). PCR primer sequences are listed in Table 1.

Western blot, immunohistochemistry and IF assays

Western blot assay

Total proteins of cells or tissues were separated by SDS-PAGE and transferred from gel to nitrocellulose membrane (GE Healthcare). Finally, after antibody incubation, the signals of detected proteins were measured by ImageQuant LAS 4000 mini (GE Healthcare) with the West-Dura detection system (Thermo) (GAPDH antibody dilution, 1:5000; other antibodies dilution, 1:1000).

Immunohistochemistry assay

Immunohistochemistry (IHC) assay of the pancreas was performed according to the manufacturer's protocol (Boster Bio-engineering Company, China, Wuhan). Tissue slides were observed under microscope. The intensity of insulin-positive signals in the pancreas was measured using Image-Pro software (insulin antibody dilution, 1:100).

IF assay

In the assays to detect IRS2, cleaved Caspase 3 and insulin, all sections were subjected to immunological reactions using standard IF procedures. After deparaffination and rehydration, antigen retrieval of 5 µm paraffin-embedded pancreas sections was conducted in citrate buffer (pH = 6). After BSA blocking, sections were incubated with the primary antibodies (rabbit anti-IRS2 and cleaved Caspase 3 antibody, diluted 1:300; mouse anti-insulin antibody, diluted 1:200) overnight at 4°C, followed by incubation with the secondary antibody (goat anti-rabbit CY3 for IRS2 and cleaved Caspase 3, goat anti-mouse Alexa 488 for insulin, diluted 1:1000) for 50 min at room temperature without light. Finally, sections were counterstained with DAPI in the dark. Before the secondary antibody incubation and DAPI staining, washing steps with PBS (pH = 7.4) were needed.

All images were collected using Nikon Eclipse C1 microscope in parallel under the same settings, including identical camera, microscope lens, light and other parameters settings. Analysis of fluorescence intensity was performed using ImageJ software with identical image

Table 1 List of rat primer sequences used in RT-PCR assay.

Gene	**Forward primer** (5′–3′)	**Reverse primer** (5′–3′)
Irs2	AGCTGGTGGTAGTCATACCC	CAGGTTCATATAGTCAGA
p21	CAAAGTATGCCGTCGTCTGT	GTCTCAGTGGCGAAGTCAAA-3
Bim	CCAGGCCTTCAACCATTATCTC	GCGCAGATCTTCAGGTTCCT
Gpr40	ACCAGTTCCCTGGGCATCAACATA	ACCAAGGGCAGAAAGAAGAGCAGA
Gapdh	TTCCAGGAGCGAGATCCCGCTAAC	CATGAGCCCTTCCACGATGCCAAAG

https://joe.bioscientifica.com
https://doi.org/10.1530/JOE-18-0432

processing procedure, and all the parameters in the image processing were consistent.

Caspase 3 and Caspase 9 activity assay

INS-832/13 cells were cultured in white opaque 96-well plates (4×10^4 cells/well) and grown overnight. The activity of Caspase 3 or Caspase 9 in cells treated with corresponding compounds was detected by applying Apo-ONE Homogeneous Caspase-3/7 Assay and Caspase-Glo 9 Assay kit (Promega).

Luciferase reporter assay

HEK293T cells were seeded in 48-well plates (5×10^4 cells/well) and cultured overnight. And transient transfection was then performed by Calcium Phosphate Cell Transfection kit (Beyotime) according to the manufacturer's protocol. After transfection, cells were incubated with the relevant compounds. Finally, cells were harvested and firefly-Renilla luciferase activities were detected using the dual-luciferase reporter assay system kit (Promega).

Intracellular cAMP assay

The content of cAMP in INS-832/13 cells was tested by using the cAMP-Glo assay kit (Promega) according to the manufacturer's protocol with a reciprocal relationship between cAMP concentration and light output observed.

Fluorescence imaging plate reader (FLIPR) assay

Cytosolic Ca^{2+} was measured using FlexStation 3 (Molecular Devices, Sunnyvale, CA, USA) to constantly monitor fluorescence signals (494 nm/525 nm) after pre-incubation with Fluo-4 AM (2 μM, Invitrogen), for 40–50 min. Ca^{2+} dynamics in cells was observed when HBSS buffer (137.93 mM NaCl, 5.33 mM KCl, 4.17 mM $NaHCO_3$, 1.26 mM $CaCl_2$, 0.493 mM $MgCl_2$, 0.407 mM $MgSO_4$, 0.441 mM KH_2PO_4, 0.338 mM Na_2HPO_4, 5.56 mM D-Glucose) containing test compounds were added into wells automatically. The whole detection lasted for 60–120 s with 1.6-s interval.

GSIS assay

INS-832/13 cells were plated into 24-well plates (2×10^5 cells/well) and incubated overnight. The cells were maintained for 2 h in Krebs-Ringer bicarbonate buffer (115 mM NaCl, 5 mM KCl, 24 mM $NaHCO_3$, 2.5 mM $CaCl_2$, 1 mM $MgCl_2$, 10 mM HEPES, pH 7.2) supplemented with 0.2% (w/v) BSA and then further incubated for 2 h with 2.8 mM or 16.8 mM glucose containing indicated compounds. Insulin content was measured with the AlphaLISA insulin kit (PerkinElmer).

Enzymatic activity assay

PI3K activity assay

PI3K activity was measured using the PI3K activity ELISA kit (Echelon, Salt Lake City, UT, USA) according to the manufacturer's protocol.

Glucokinase (GK) activity assay

GK activity was detected according to the previous study (Grimsby *et al.* 2003). Briefly, the reaction was initiated by the addition of 10 μL ATP (10 mM) in the assay solution (25 mM HEPES, 25 mM KCl, 2 mM $MgCl_2$, 1 mM ATP, 1 mM DTT, 1 mM NAD, 0.1% (w/v) BSA, 5 units/mL glucose-6-phosphate dehydrogenase (G6PDH), 5 mM glucose and 18.7 mg/mL hLGK2, pH 7.1) to produce NADH, and then the absorbance was measured at 340 nm using FlexStation 3 (Molecular Devices).

PDE activity assay

PDE activity assay was applied using the PDE Activity Assay Kit (Abcam) according to the manufacturer's protocol.

GPR40 activity assay

Activation of compounds on GPR40 was regarded as the change of Ca^{2+} flow in hGPR40-CHO cells; thus, this assay was performed as FLIPR assay.

Cellular thermal shift assay (CETSA)

INS-832/13 cells were grown in culture dishes until cell density achieved 80–90%. Cells were homogenized in RIPA buffer containing protease and phosphatase inhibitor cocktail at 4°C for 15 min and then broken completely by a sonicator on ice. The homogenates were then centrifuged (13,400 ***g***, 30 min, 4°C) to harvest cell supernatant. After dividing into two groups treated with test compounds and vehicle respectively, these lysates were heated at a series of gradient temperature. All heated samples were centrifuged (13,400 ***g***, 2 h, 4°C) again to collect soluble proteins. After mixing with 5× SDS-PAGE loading buffer and being heated for 10 min at 99°C, these proteins were analyzed by Western blot.

https://joe.bioscientifica.com
https://doi.org/10.1530/JOE-18-0432

siRNA transfection

INS-832/13 cells were transfected using Lipofectamine RNAiMAX (Invitrogen) according to the manufacturer's protocols and non-targeting siRNA (Invitrogen) was used as a negative control. Expressions of analytes were detected by qRT-PCR and Western blot.

Plasmid construction and transient transfection of cells

The GPR40-overexpression plasmid was constructed by introducing the insertion of GPR40-cDNA into plasmid vector p3×FLAG-myc-CMV-24 (Sigma). The constructed plasmids were transfected in INS-832/13 cells using Lipofectamine 3000 (Invitrogen) according to the manufacturer's protocols and the empty vector was used as a negative control.

Animal experiment

All animals received human care and were bred at 20–25°C with 50% relative humidity, a 12:12 light/darkness cycle and water and food *ad libitum*. Animal experiments were approved by the Institutional Animal Care and Use Committee, Shanghai Institute of Materia Medica, Chinese Academy of Sciences.

db/db male and female mice (BKS.Cg-*Dock7*$^{m+/+}$*Lepr*^{db}/J) were from Jackson Laboratory. HFD/STZ-induced type 2 diabetic model mice were constructed with reference to the published reports (Ito *et al.* 1999, Deeds *et al.* 2011). After 4-week HFD diet (containing 58% fat), 6-week-old male mice were intraperitoneally injected with a single 100 mg/kg STZ. Diabetic model mice were screened by detecting 6-h fasting blood glucose after 3 days, and they were assigned randomly to three groups according to blood glucose level and body weight ($n=9$). Vehicle (physiological saline) and 15 or 30 mg/kg vincamine hydrochloride (as vincamine) were administered daily by intraperitoneal (i.p.) injection for 5–6 weeks. Diet and body weight were monitored throughout the whole experimental process. Fasting blood glucose levels of all mice were measured weekly after 6-h fasting each time. At the fourth week, oral glucose tolerance test (OGTT) (1.0 g/kg glucose) was carried out after overnight fasting. Blood samples from tail veins were collected to determine glucose and insulin levels. Insulin content in serum was determined by the AlphaLISA insulin kit (PerkinElmer). At the fifth week, i.p. insulin tolerance test (ITT) (1.5 U/kg) on *db/db* female mice was carried out after 6-h fasting. At the end of the experiment, mice were killed and tissues were stored at −80°C for further analysis.

Statistical analysis

Data are presented as mean ± S.E.M. The two-tailed unpaired *t*-test was used to test differences between two groups and one-way ANOVA was performed to compare among three groups or more. The data analyses of fasting blood glucose test and OGTT and ITT were done using two-way ANOVA, and two independent variables included treatment (vehicle or vincamine) and time.

Results

Vincamine improves β-cell dysfunction

MTT assay

To investigate the potential protection of vincamine against β-cell damage, 3-(4,5-dimethylthiazol-2-yl)-2,5-diphenyl-tetrazolium bromide (MTT) assay was carried out in INS-832/13 cells with or without STZ (0.4 mM) stimulus (Zheng *et al.* 2015). As shown in Fig. 1B and C, vincamine (Vin) itself had no effect on INS-832/13 cells viability, whereas it could counteract the STZ-induced decrease in cell viability by EC_{50} at 5.78 μM (Fig. 1C). These data suggested that vincamine enhanced INS-832/13 cells viability under STZ treatment.

Apoptosis assay

Given that Annexin V labeled with a fluorescent signal is routinely used to effectively detect apoptotic cells (Medarova *et al.* 2005), we performed flow cytometry (FCM) analysis of Annexin V-FITC/PI double staining to further investigate the protective effect of vincamine on INS-832/13 cells. As shown in Fig. 1D, vincamine efficiently decreased the mass of apoptotic cells induced by STZ (0.4 mM). Since STZ could not stimulate cell necrosis at 0.4 mM (Saini *et al.* 1996), the effect of vincamine on cell necrosis was beyond our investigation. Thus, we determined that vincamine improved INS-832/13 cells dysfunction against the STZ-induced apoptosis.

Proliferation assay

Considering that anti-apoptosis and stimulation of proliferation are both pivotal for ameliorating β-cell dysfunction (Vetere *et al.* 2014), we next detected the effect of vincamine on β-cell proliferation in INS-832/13 cells. As illustrated in Fig. 1E (liraglutide as a positive

https://joe.bioscientifica.com
https://doi.org/10.1530/JOE-18-0432

control (Tamura *et al.* 2015)), vincamine exhibited no effect on INS-832/13 cell proliferation.

Therefore, all results demonstrated that vincamine exhibited capability in protecting against the STZ-induced apoptosis of β-cells.

Vincamine protects β-cells by regulating IRS2/PI3K/Akt signaling

Given that Akt is a key protein involved in the signaling transductions of β-cell growth and apoptosis and Akt1-deficient mice result in β-cell dysfunction similar to those observed in T2DM (Bernal-Mizrachi *et al.* 2004), we next investigated the potential regulation of vincamine against Akt signaling.

Vincamine reversed the STZ-induced reduction of p-Akt

Considering that AlphaLISA is a bead-based immunoassay with high selectivity and sensitivity (Bielefeld-Sevigny 2009), we at first performed an AlphaLISA-based assay to investigate the potential of vincamine in stimulating p-Akt. As expected, vincamine antagonized the STZ-induced decrease in p-Akt by EC_{50} at 3.92 μM in INS-832/13 cells (Fig. 2A).

Next, Western blot assay was also applied to further verify AlphaLISA results. As indicated in Fig. 2B, vincamine had no effect on p-Akt but could recover the STZ-induced reduction of p-Akt in INS-832/13 cells.

Thus, all above-mentioned results have demonstrated that vincamine exhibited capability in reversing the STZ-induced reduction of p-Akt in β-cells.

Vincamine promoted β-cell survival involving PI3K/Akt signaling

Considering that PI3K is one of the most common regulators of Akt in response to cell survival and growth (Khorami *et al.* 2015), we next detected whether the vincamine-mediated β-cell survival and p-Akt restoration were of PI3K dependence. As indicated in Fig. 2C and Supplementary Fig. 1A, D (see section on supplementary data given at the end of this article), MTT and FCM assay result demonstrated that wortmannin (PI3K inhibitor) could largely impede the activity of vincamine in reversing the STZ-induced cell apoptosis, and Western blot result (Fig. 2D) also verified the preclusion of wortmannin against the antagonism of vincamine in the STZ-induced p-Akt inhibition. Obviously, vincamine could efficiently recover the STZ-induced decrease in p-PI3K (Fig. 2E).

Next, by considering that effectors, such as FOXO1, GSK3β, Caspase 9, Bim and p21 in the downstream of PI3K/Akt pathway, are vital in anti-apoptosis (Elghazi & Bernal-Mizrachi 2009), we assayed the regulation of vincamine against these downstream effectors of PI3K signaling. The results indicated that vincamine could reverse the STZ-induced decrease in phosphorylated FOXO1 (Ser 256)/GSK3β (Ser 9) (Fig. 2E) and deplete the STZ-induced increases in enzyme activity of Caspase 9/3 (Fig. 2F and G) and protein level of cleaved Caspase 3 (Fig. 2H), while it also decreased the elevation of Bim and p21 mRNA stimulated by STZ (Fig. 2I and J).

Thus, all above-mentioned results demonstrated that PI3K/Akt signaling was involved in the vincamine-induced β-cell survival.

IRS2 was in the upstream of PI3K/Akt signaling responding to vincamine regulation

As reported, PI3K signaling modulation may involve any of the following events: (1) direct ligand for PI3K can regulate its enzymatic activity (Ikeda *et al.* 2010); (2) LXR regulates PI3K by activating the key components of PI3K signaling (Huwait *et al.* 2015); (3) insulin receptor substrate 2 (IRS2) acts as an interface between activated tyrosine kinase receptors and downstream signaling molecules including PI3K (Oliveira *et al.* 2014). Thus, we carried out the relevant assays to investigate the upstream of PI3K/Akt signaling in response to vincamine regulation. As demonstrated in Fig. 2K and L, vincamine antagonized the STZ-induced decrease of IRS2 in either mRNA or protein level in INS-832/13 cells but rendered no effect on PI3K enzyme activity (Supplementary Fig. 2A) or LXRα/β (Supplementary Fig. 2B and C).

Taken together, IRS2 was in the upstream of PI3K/Akt signaling responding to vincamine regulation.

cAMP and Ca^{2+} participate in vincamine protecting against STZ-induced β-cell apoptosis

As IRS2/PI3K/Akt signaling has been indicated to be involved in the vincamine-mediated β-cell protection and a published report has indicated that IRS2 is mediated by cAMP or Ca^{2+}-regulated transcription factors in β-cells (Kuznetsova *et al.* 2016), we next investigated whether regulation of vincamine involved these two second messengers in INS-832/13 cells.

Vincamine protected β-cells by involving regulation of Ca^{2+}

Intracellular Ca^{2+} measurement was performed in INS-832/13 cells by FlexStation 3 to constantly monitor

https://joe.bioscientifica.com
https://doi.org/10.1530/JOE-18-0432

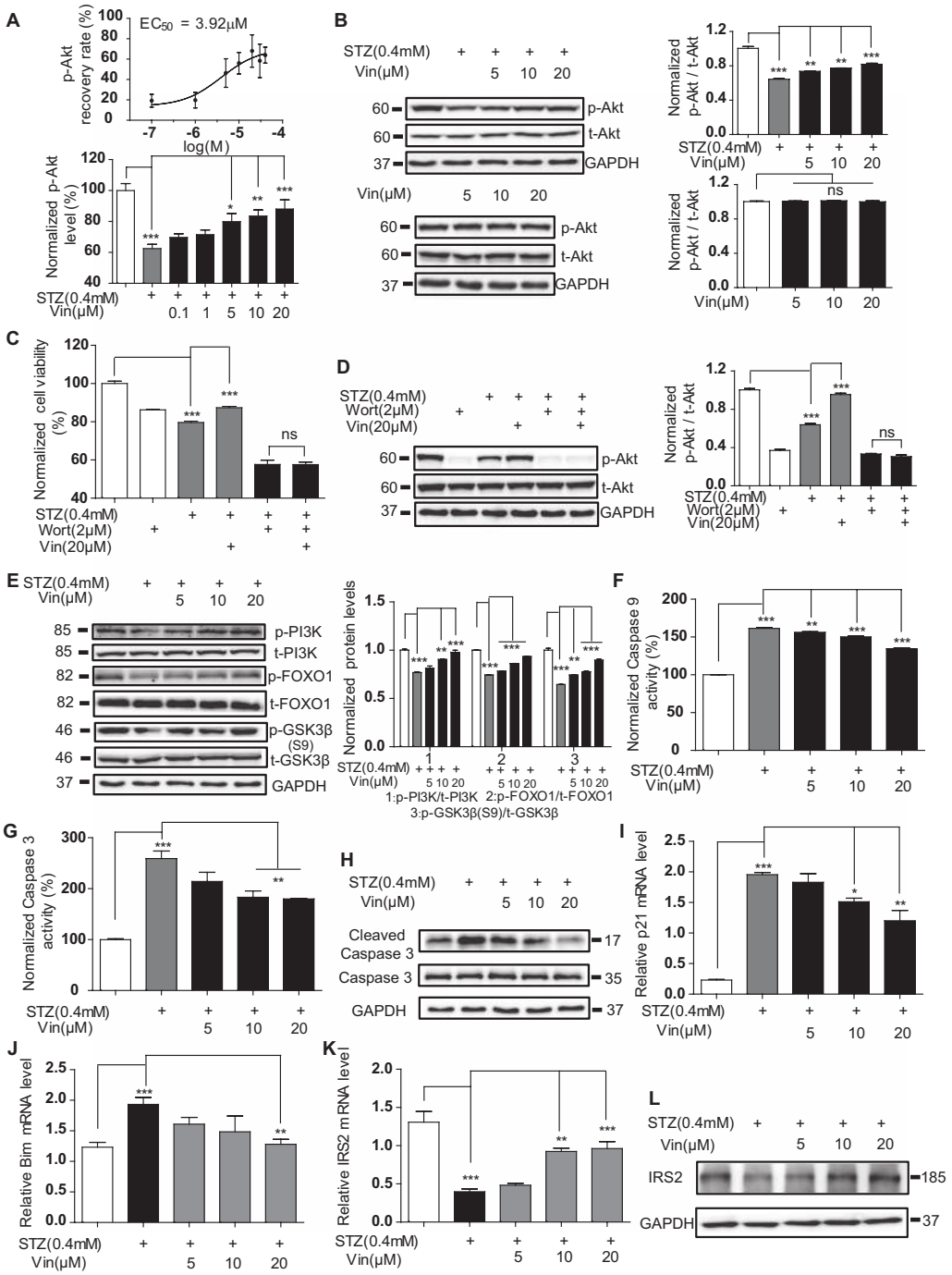

Figure 2

Vincamine protects β-cells through IRS2/PI3K/Akt pathway. (A) After incubation with STZ (0.4 mM) and vincamine (0.1, 1, 5, 10, 20 μM) in INS-832/13 cells for 24 h, the level of p-Akt was determined by AlphaLISA assay. Vincamine-EC_{50} of p-Akt recovery was fitted by GraphPad Prism. (B) INS-832/13 cells with or without STZ treatment were incubated with vincamine (5, 10, 20 μM) for 24 h, and then p-Akt was detected by Western blot. (C) In the presence of wortmannin (2 μM), vincamine-induced β-cell survival was measured as in Fig. 1C. (D) The level of p-Akt was detected by Western blot in INS-832/13 cells incubated with STZ (0.4 mM) and vincamine (20 μM) for 24 h in the presence of wortmannin (2 μM). (F, G and H) INS-832/13 cells were incubated with STZ (0.4 mM) and vincamine (5, 10, 20 μM) for 6 h, and then the activity of Caspase 9 (F) and Caspase 3 (G) were examined using corresponding assay kits and the expression of cleaved Caspase 3 (H) was detected by Western blot. (E, I, J, K and L) INS-832/13 cells were treated with STZ (0.4 mM) and vincamine (5, 10, 20 μM) for 24 h. IRS2/PI3K/Akt pathway-related proteins (E, L) were then assessed by Western blot, and the mRNA expressions of p21 (I), Bim (J) and IRS2 (K) were detected by quantitative real-time PCR (qRT-PCR). Data were shown as means ± S.E.M. with three independent experimental replicates. Significant differences between groups are represented as $*P < 0.05$, $**P < 0.01$ and $***P < 0.001$ and $P > 0.05$ meant no significance (ns). (Vin, as vincamine; Wort, as wortmannin.)

https://joe.bioscientifica.com
https://doi.org/10.1530/JOE-18-0432

fluorescence signals. As indicated in Fig. 3A and B, vincamine increased Ca^{2+} influx and such an increase was eliminated by depleting extracellular Ca^{2+} in HBSS buffer (Fig. 3C and D) or in the presence of nifedipine (inhibitor of L-type VDCCs) (Fig. 3E). In addition, nifedipine could also block the activity of vincamine in either protecting against the STZ-induced INS-832/13 cell apoptosis or reversing the STZ-induced decrease in p-Akt or IRS2 level (Fig. 3F, G and Supplementary Fig. 1B, E).

These results thereby demonstrated that vincamine protected β-cell by involving Ca^{2+} influx.

cAMP signaling was required for vincamine-induced β-cell protection

Next, we investigated the potential regulation of vincamine against cAMP level in INS-832/13 cells. The results demonstrated that vincamine incubation obviously enhanced cAMP level in cells similar to those of FSK (adenylyl cyclase activator) as a positive control (Fig. 3H), and the protection of vincamine against the cells was inhibited by the presence of MDL-12,330A hydrochloride (MDL, adenylyl cyclase inhibitor) or H89 (PKA inhibitor) (Fig. 3I and Supplementary Fig. 1B, E). Moreover, the results that H89 blocked the vincamine-stimulated increase in p-Akt or IRS2 level in STZ-treated INS-832/13 cells (Fig. 3J) served a further demonstration that cAMP pathway participated in this process.

Therefore, these results indicated that cAMP/IRS2/PI3K/Akt signaling was involved in the vincamine-mediated β-cell protection.

Vincamine-mediated Ca^{2+} influx was in a cAMP-dependent manner

Given the capacity of vincamine in regulating Ca^{2+} influx and cAMP, we next investigated their affiliations in this event. It is noted that reciprocal regulation between Ca^{2+} and cAMP is intricate, while cAMP and PKA influence Ca^{2+} at nearly every level including the generation and termination of Ca^{2+} (Hofer 2012). Furthermore, pancreatic β-cell voltage-gated calcium channel can be regulated by cAMP signaling (Leiser & Fleischer 1996, Yang & Berggren 2006). With these facts, we thus tentatively suppose that cAMP might be in the upstream of Ca^{2+} influx in response to vincamine regulation. To verify such a presumption, after blocking cAMP pathway, the changes of Ca^{2+} influx in INS-832/13 cells were detected. As indicated in Fig. 3K, these above-mentioned changes could be totally eliminated by MDL.

Therefore, all results demonstrated that cAMP/Ca^{2+} were in the upstream of IRS2/PI3K/Akt pathway, which was responsible for the protection of vincamine against STZ-induced β-cell apoptosis.

Vincamine promotes GSIS by regulating cAMP and CaMKII signaling

As we have determined that cAMP and Ca^{2+} play a vital role in vincamine regulation and GSIS as a potent physiological process is tightly associated with kinases via various signaling pathways, including PKA via Ca^{2+}-dependent cAMP production, Ca^{2+} and calmodulin-dependent protein kinase II (CaMKII) (Dall'Asta *et al.* 2015), we next investigated the potential of vincamine in regulating GSIS in INS-832/13 cells using glibenclamide (diabetic drug) as a positive control.

Vincamine promoted GSIS

As shown in Fig. 4A, vincamine effectively promoted GSIS in cells with a high concentration of glucose (16.8 mM) (Kong *et al.* 2014) rather than with low concentration of glucose (2.8 mM).

Next, we explored the mechanism underlying the regulation of vincamine against GSIS in INS-832/13 cells. We found that treatment of nifedipine or 2-APB (a manipulator of intracellular Ca^{2+} release) failed to deprive the ability of vincamine promoting GSIS (Fig. 4B and Supplementary Fig. 3), and either MDL (Fig. 4C) or KN62 (CaMKII inhibitor, Fig. 4D) incubation could effectively hinder the promotion of vincamine on GSIS, which suggested that cAMP and Ca^{2+}/CaMKII pathways participated in vincamine-promoted GSIS.

Therefore, all results supported that cAMP/Ca^{2+}/CaMKII signaling is required for the vincamine-induced promotion on GSIS.

Vincamine protected β-cells regardless of insulin secretion promotion

Additionally, given the strong effect of vincamine on GSIS, we next detected whether this effect contributed to vincamine-mediated β-cell protection. As shown in Supplementary Fig. 4, vincamine rendered no effect on stimulating insulin secretion in STZ-treated INS-832/13 cells. Thus, the protective effect of vincamine on β-cells was not related to vincamine-promoted insulin secretion.

Vincamine protects β-cells and enhances GSIS by functioning as a GPR40 activator

As vincamine was capable of promoting both β-cell survival and GSIS and the related mechanisms have

https://joe.bioscientifica.com
https://doi.org/10.1530/JOE-18-0432

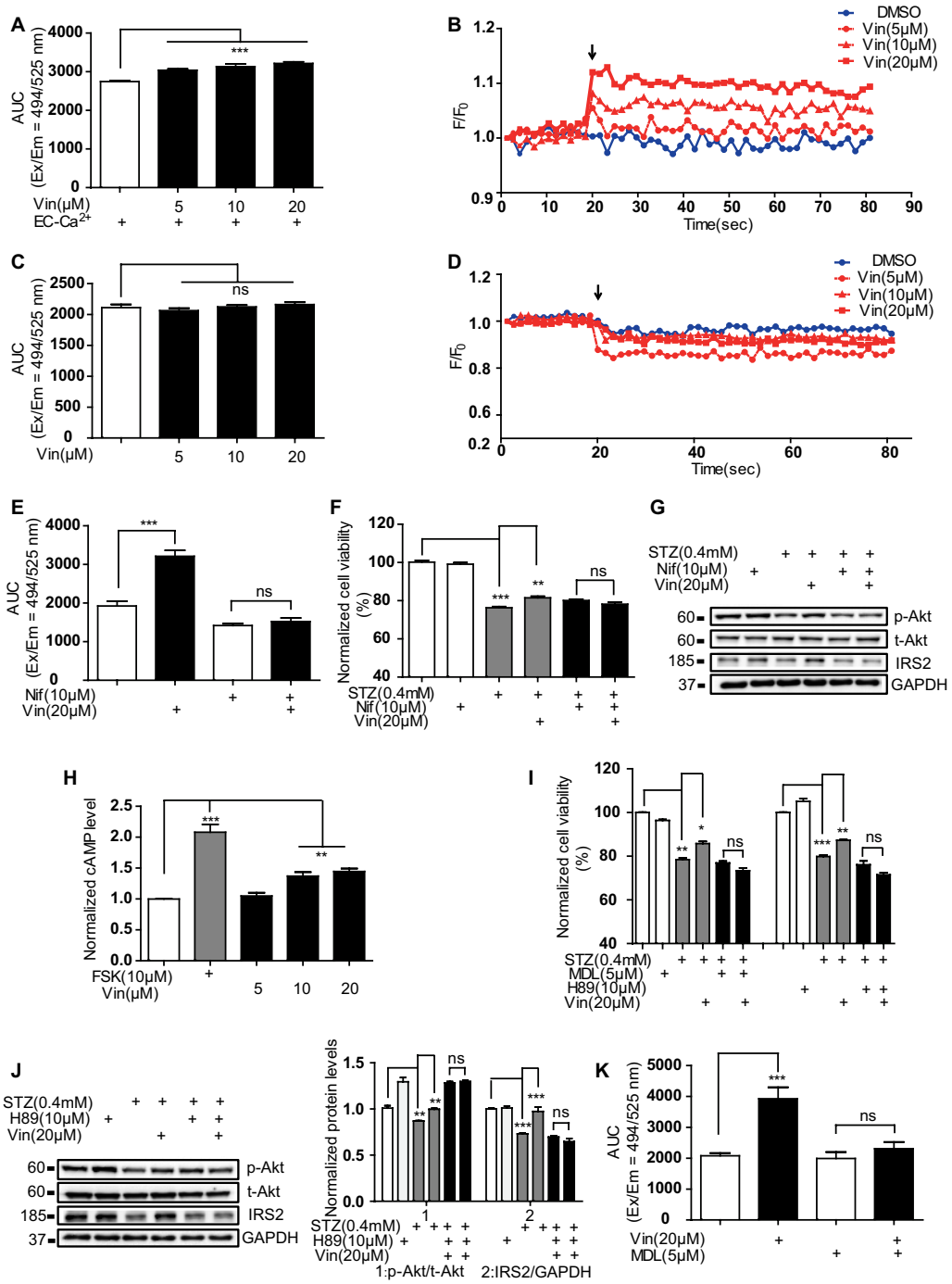

Figure 3

cAMP and Ca^{2+} contribute to vincamine-induced β-cell protection. (A, B, C and D) Cytosolic Ca^{2+} signals in INS-832/13 cells were measured using Fluo-4 AM. Vincamine (5, 10, 20 μM) was added into INS-832/13 cells automatically, and Ca^{2+} signal in the first 20 s of detection was set as the baseline signal. Ca^{2+} signal assay was carried out in the presence (A) or absence (C) of extracellular Ca^{2+}, and data were presented as AUC form. (B and D) B and D were the real-time Ca^{2+} dynamics of A and C respectively. (E) After pre-incubation with nifedipine (10 μM), Ca^{2+} signal was detected as in A. (F) In the presence of nifedipine (10 μM), the viability of INS-832/13 cells was examined as in Fig. 1C. (G and J) The expressions of p-Akt and IRS2 were detected as in Fig. 2B under the treatment with nifedipine (10 μM) (G) and H89 (10 μM) (J). (H) INS-832/13 cells were treated with FSK (10 μM) or vincamine (5, 10, 20 μM) for 1 h, and concentration of intracellular cAMP was detected using assay kit. (I) Viability of INS-832/13 cells was examined as in Fig. 1C in the presence of H89 (10 μM) and MDL-12,330A hydrochloride (MDL, 5 μM). (K) Ca^{2+} signal was detected as in A in the presence of MDL (5 μM). Data were shown as means ± S.E.M. with three independent experimental replicates. Significant differences between groups are represented as $^{*}P < 0.05$, $^{**}P < 0.01$ and $^{***}P < 0.001$, and $P > 0.05$ meant no significance (ns). (EC-Ca^{2+}, as Extracellular Ca^{2+}; Nif, as Nifedipine; Vin, as vincamine.)

https://joe.bioscientifica.com
https://doi.org/10.1530/JOE-18-0432

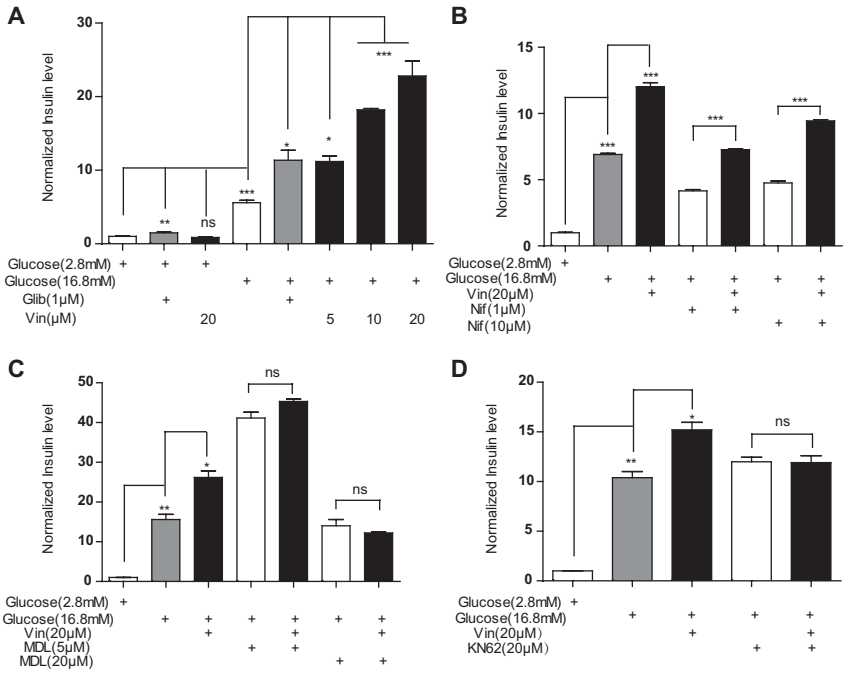

Figure 4
Vincamine induces GSIS through cAMP/Ca^{2+}/CaMKII pathway. (A) INS-832/13 cells were stimulated with 2.8 or 16.8 mM glucose in the presence of glibenclamide (1 μM) or vincamine (5, 10, 20 μM) for 2 h, and the supernatant of cells was then harvested to detect insulin content. (B, C and D) Insulin content was analyzed as in A when INS-832/13 cells were incubated with nifedipine (1, 10 μM) (B), MDL (5, 20 μM) (C) and KN62 (20 μM) (D). Data were shown as means ± S.E.M. with three independent experimental replicates. Significant differences between groups are represented as $*P < 0.05$, $**P < 0.01$ and $***P < 0.001$ and $P > 0.05$ meant no significance (ns). (Glib, as glibenclamide; Nif, as nifedipine; Vin, as vincamine.)

been also investigated, we next explored the potential target of vincamine.

According to the published reports, cytosolic Ca^{2+} can be regulated by GK in pancreatic β-cells, and cAMP may be controlled by phosphodiesterase (PDE) that is highly expressed in β-cells (Zhao *et al*. 2014, Markwardt *et al*. 2016). Moreover, G protein subunits regulate G protein-coupled signaling pathways involving the secondary messengers (e.g. cAMP and Ca^{2+}) that ultimately control biosynthesis, secretion, proliferation and anti-apoptotic pathways of pancreatic islets (Moran *et al*. 2016). In addition, vincamine was once verified as an NMDAR antagonist in the nervous system (Kaneko *et al*. 1991), and inhibition of NMDARs in islets has been reported as a strategy for enhancing GSIS and β-cell survival (Marquard *et al*. 2015). We next investigated whether vincamine targeted the above-mentioned signaling pathways.

Vincamine had no effect on GK, PDE and NMDAR

We detected the effect of vincamine on either of the enzyme activities of GK and PDE and also tested the effect of vincamine on β-cell protection in the presence of t-PDC (Marquard *et al*. 2015) (EAAT inhibitor, l-*trans*-pyrrolidine-2,4-dicarboxylate) and NMDA (agonist of NMDAR). As shown in Fig. 5A, B and C, vincamine had no impact on either of the enzyme activities of GK and PDE, and NMDA rendered no effect on the protection of vincamine against INS-832/13 cells in the presence of t-PDC.

Vincamine activated GPR40

We examined the potential of vincamine in regulating GPR40 by FLIPR approach, since GPR40 activation triggers intracellular Ca^{2+} enhancement (Hu *et al*. 2009). As expected, vincamine could activate GPR40 (EC_{50} = 6.28 μM) with DHA (GPR40 ligand) (Itoh *et al*. 2003) as a positive control (EC_{50} = 3.85 μM) in hGPR40-CHO cells (Fig. 5D).

CETSA confirmed vincamine binding to GPR40

CETSA is a recently developed approach to examine the ligand-induced thermal shift of target protein in cells, tissues or cell lysates (Molina *et al*. 2013). CETSA was performed by heating the compound-treated cell lysates, followed by elimination of the cell pellet and detection of the remaining target protein (Jafari *et al*. 2014). Here, we used CETSA to assess the binding of vincamine to GPR40 in INS-832/13 cells. As indicated in the gradient heating results (TAK-875 as a positive control, Srivastava *et al*. 2014), GPR40 in the vincamine-treated cell lysate showed better stability than the DMSO-treated group, and vincamine rendered no influence on the denaturing temperatures of other proteins as control, such as Akt, GSK3β and GAPDH (Fig. 5E and Supplementary Fig. 5A, B). All results thus implied the specific affinity of vincamine to GPR40.

Therefore, combining with the above-mentioned result that vincamine-stimulated GPR40 activity, we suggested that vincamine functioned as a GPR40 activator.

https://joe.bioscientifica.com
https://doi.org/10.1530/JOE-18-0432

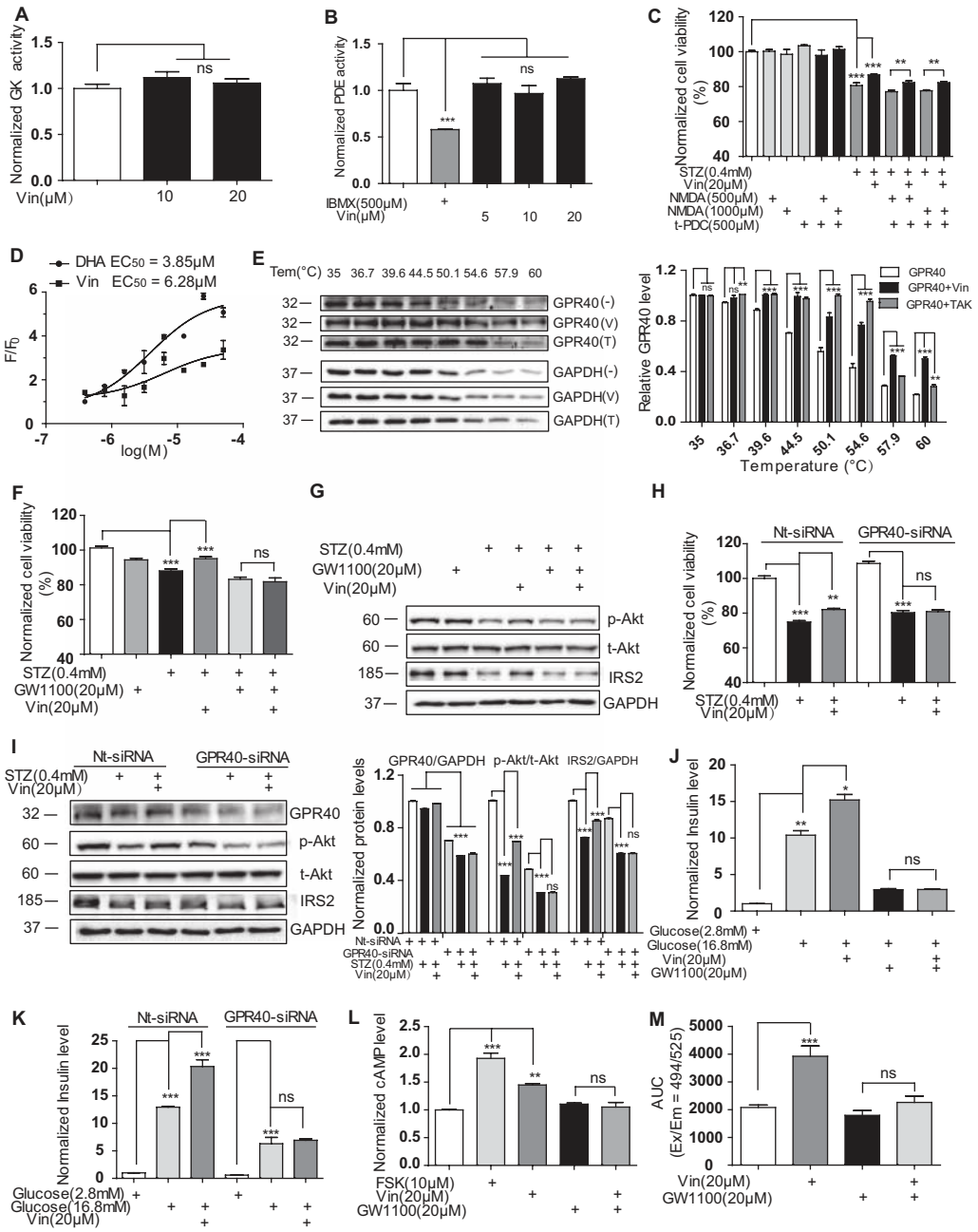

Figure 5

Vincamine ameliorates β-cell function and promotes GSIS by targeting GPR40. (A) GK enzymatic activity was tested with the treatment of vincamine (10, 20 μM). (B) The enzymatic activity of PDE was assessed when incubated with IBMX (500 μM) or vincamine (5, 10, 20 μM). (C) After treatment with NMDA (500, 1000 μM) and t-PDC (500 μM), the viability of INS-832/13 cells was detected as in Fig. 1C. (D) Vincamine and DHA in different concentrations were added into hGPR40-CHO cells pre-incubated with Fluo-4 AM, and Ca^{2+} signals were recorded. (E) CETSAs for INS-832/13 cell lysate treated with DMSO and vincamine (20 μM) or TAK-875 (20 μM) were conducted using Western blot to detect the interaction between vincamine and GPR40, and quantification of this data was also shown in E. (F) After incubation with GW1100 (20 μM), the viability of INS-832/13 cells was detected as in Fig. 1C. (G) Expressions of p-Akt and IRS2 were examined as in Fig. 2B in the presence of GW1100 (20 μM). (H) After transfection with non-targeting siRNA or GPR40-siRNA (100 pM), the viability of INS-832/13 cells was detected as in Fig. 1C. (I) Detection of GPR40, p-Akt and IRS2 expression was conducted by Western blot under the same condition as in H. (J and K) The insulin content was detected as in Fig. 4A after treatment with GW1100 (20 μM) (J) and transfection with non-target siRNA or GPR40-siRNA (100 pM) (K). (L) Intracellular cAMP concentration was determined as in Fig. 3H under GW1100 (20 μM) treatment. (M) Ca^{2+} mobilization was measured as in Fig. 3A in the presence of GW1100 (20 μM). Data were shown as means ± S.E.M. with three independent experimental replicates. Significant differences between groups are represented as $^{*}P < 0.05$, $^{**}P < 0.01$ and $^{***}P < 0.001$, and $P > 0.05$ meant no significance (ns). ((–): with DMSO; Nt-siRNA, as non-targeting siRNA; (V): with vincamine; Vin, as vincamine; (T): with TAK-875; TAK, as TAK-875.)

https://joe.bioscientifica.com
https://doi.org/10.1530/JOE-18-0432

GPR40 was required for the vincamine-mediated β-cell protection or GSIS promotion

Next, we investigated whether vincamine protected β-cells and promoted GSIS by targeting GPR40 in INS-832/13 cells.

The transfection effectiveness of GPR40 siRNA was examined by qRT-PCR and Western blot (Supplementary Fig. 6A and B).

As indicated in Fig. 5F, G, H, I and Supplementary Fig. 1A, C, D, F, either treatment of GW1100 (a selective GPR40 inhibitor) or GPR40 siRNA could efficiently block the capability of vincamine in either protecting against the STZ-induced INS-832/13 cells apoptosis or stimulating p-Akt and IRS2 levels.

Similarly, assays by treatment with GW1100 and GPR40 siRNA were also performed to evaluate the promotion of vincamine on GSIS by targeting GPR40. As shown in Fig. 5J and K, the weakened capacity of vincamine in stimulating GSIS in the presence of GW1100 or by GPR40 siRNA transfection suggested that vincamine stimulated GSIS in a GPR40-dependent manner. Moreover, GW1100 treatment could also deprive the ability of vincamine in promoting Ca^{2+} and cAMP levels (Fig. 5L and M).

In addition, we performed a series of assays in GPR40-overexpressed INS-832/13 cells to verify GPR40-mediated events in β-cells. The transfection effectiveness of GPR40-overexpression plasmid was verified by Western blot (Supplementary Fig. 7A). As shown in Supplementary Fig. 7B, C and D, transfection of GPR40-overexpression plasmid could ameliorate STZ-induced INS-832/13 cells viability reduction and STZ-induced increases in enzyme activity of Caspase 3 and protein level of cleaved Caspase 3. Moreover, insulin secretion at 16.8 mM glucose incubation, cAMP level and Ca^{2+} influx could be enhanced in GPR40-overexpressed cells (Supplementary Fig. 7E, F and G). All these results demonstrated that the events triggered by GPR40 overexpression were same as the various effects of vincamine upon β-cell functions and signaling pathways, which supported that vincamine indeed triggered the activation of GPR40-mediated signaling events.

Taken together, all above results supported that vincamine protected β-cells and promoted GSIS by targeting GPR40.

Vincamine improves glucose tolerance in type 2 diabetic model mice

As we have determined the promotion of vincamine on β-cell survival and GSIS in INS-832/13 cells, we next investigated its pharmacological activity in type 2 diabetic model mice including HFD/STZ (Li *et al.* 2017) and *db/db* (Brownlee 2001) male mice. In the assays, intraperitoneal (i.p.) injection of vincamine was performed with two concentrations (15 and 30 mg/kg/day) for 5 (*db/db* male mice) or 6 (HFD/STZ mice) weeks. It was found that vincamine effectively lowered the levels of fasting blood glucose and glycated hemoglobin (HbA1c) (Fig. 6A, B, C and D), while ameliorated oral glucose tolerance and elevated glucose-induced plasma insulin concentration (Fig. 6E, F, G, H, I and J) without influence on basal insulin secretion *in vivo* (Supplementary Fig. 8A and B).

Vincamine increases pancreatic islets area in type 2 diabetic model mice

Since cell-based investigation has demonstrated the amelioration of vincamine on β-cell dysfunction, we next performed morphology assays to examine the protection of vincamine against β-cell death and the area of insulin-positive islets with vincamine administration in HFD/STZ and *db/db* male mice.

As shown in Fig. 7A, B, C and D, vincamine treatment effectively increased both area and number of pancreatic islets, as well as number of β-cells in the pancreas and also improved the integrity of islets compared with vehicle groups. Besides, vincamine might have no significant effect on the size of β-cells (Fig. 7A and B).

Vincamine regulates IRS2/PI3K/Akt signaling *in vivo*

Given the determined protection of vincamine against the STZ-induced cell apoptosis by regulating IRS2/PI3K/Akt signaling in INS-832/13 cells, we next examined such effects of vincamine in pancreatic islet tissues of HFD/STZ and *db/db* male mice.

It was found that vincamine administration in either HFD/STZ or *db/db* male mice led to increases in phosphorylation levels of PI3K, Akt, GSK3β (Ser 9) and FOXO1, and elevation in protein level of IRS2 (Fig. 8A, B, C and D), while decrease in Caspase 3 enzymatic activity (Fig. 8E and F).

Furthermore, we performed IF assay to investigate vincamine-mediated signaling pathway in islets. As shown in Fig. 8G, H, I, J, K, L, M and N, vincamine administration led to elevation in protein level of IRS2 while decrease in protein level of cleaved Caspase 3 in islets of either HFD/STZ or *db/db* male mice.

Therefore, all above results supported that vincamine-mediated signaling pathways *in vivo* occurred mainly in islets and were completely in accordance with the cell-based results.

https://joe.bioscientifica.com
https://doi.org/10.1530/JOE-18-0432

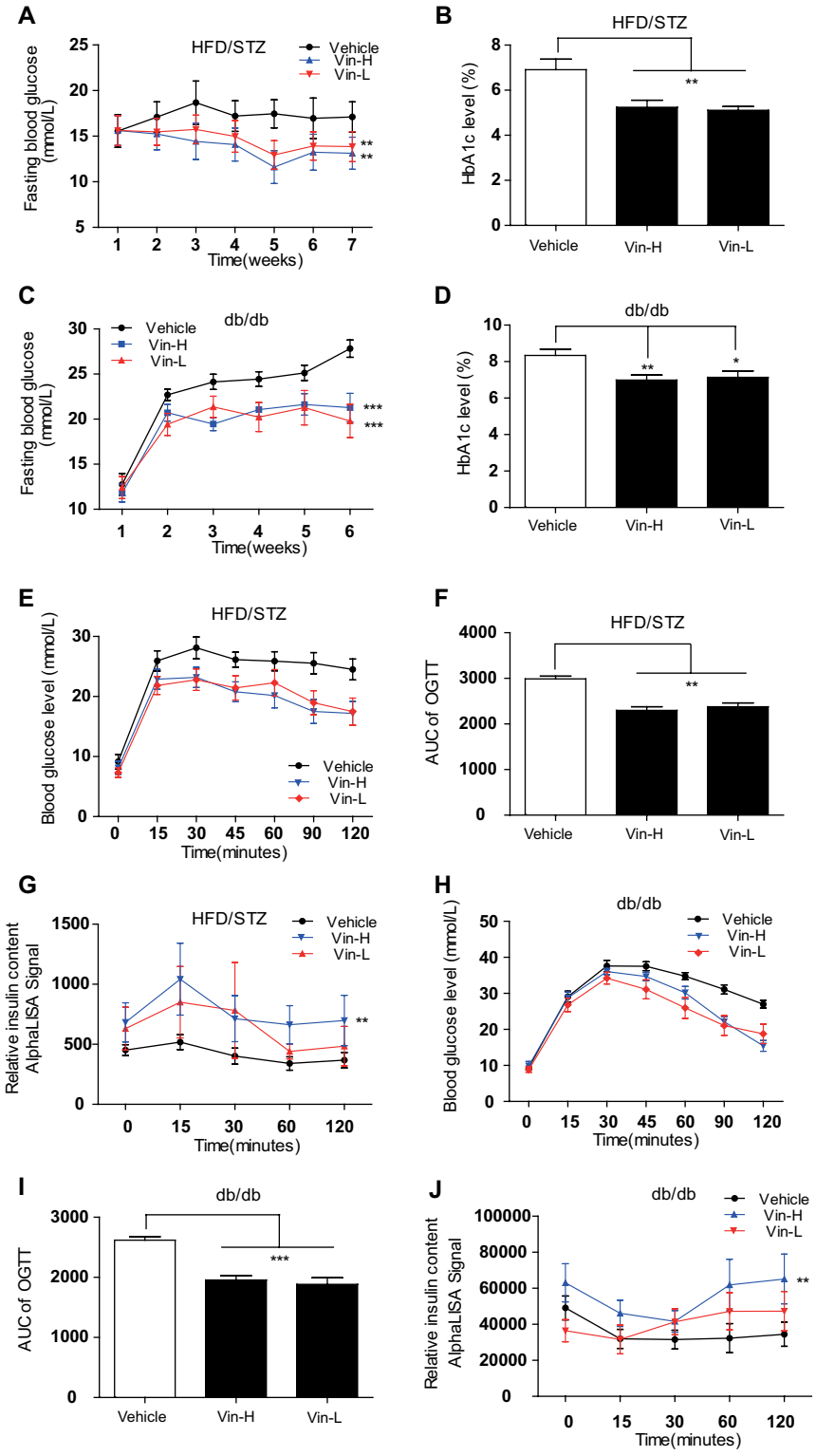

Figure 6
Vincamine administration improves glucose tolerance in HFD/STZ and *db/db* male mice. (A and C) Fasting blood glucose levels of HFD/STZ (A) and *db/db* (C) male mice were measured weekly. (Black line, vehicle; blue line, 30 mg/kg/day vincamine; red line, 15 mg/kg/day vincamine) (B and D) HbA1c levels of HFD/STZ (B) and *db/db* (D) male mice were detected after vehicle or vincamine (15, 30 mg/kg/day) administration for 5–6 weeks. (E and H) Blood glucose levels of HFD/STZ (E) and *db/db* (H) male mice during i.g. glucose (1.0 g/kg) tolerance tests with vehicle or vincamine (15, 30 mg/kg/day) treatment. (F and I) F and I were the AUC form of E and H respectively. (G and J) Serum insulin levels of HFD/STZ (G) and *db/db* (J) male mice were determined during the same process as shown in E and H. Data were shown as means ± S.E.M. with nine mice in each group. Significant differences between groups are represented as $^{*}P < 0.05$, $^{**}P < 0.01$ and $^{***}P < 0.001$. (H, 30 mg/kg/day; L, 15 mg/kg/day; Vin, as vincamine.)

Vincamine has no effect on insulin sensitivity *in vivo* and *ex vivo*

Given that administration of vincamine was able to ameliorate glucose homeostasis in either HFD/STZ or *db/db* male mice, we next detected the effect of vincamine upon insulin sensitivity *in vivo* and *ex vivo*.

In vivo, intraperitoneal (i.p.) injection of vincamine was performed with single concentration (30 mg/kg/day) on *db/db* female mice (Shi *et al.* 2013) for 6 weeks.

https://joe.bioscientifica.com
https://doi.org/10.1530/JOE-18-0432

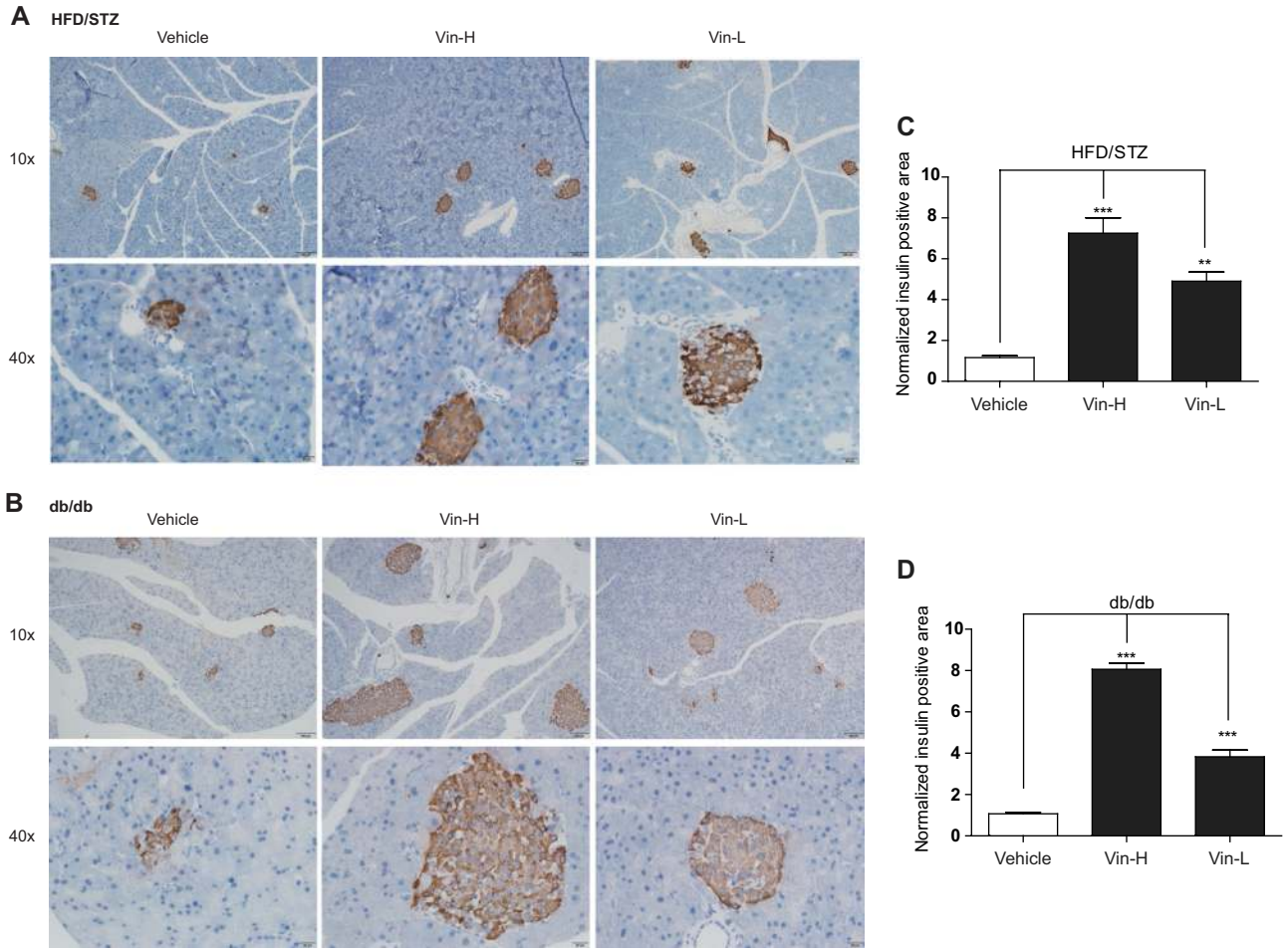

Figure 7
Vincamine administration ameliorates β-cell dysfunction and increases β-cell mass in HFD/STZ and *db/db* male mice. (A and B) Insulin IHC assays of pancreases in HFD/STZ (A) and *db/db* (B) male mice were displayed. (C) and (D) were quantitative results in insulin-positive area of pancreatic islets as shown in A and B respectively. Data were shown as means ± S.E.M. Significant differences between groups are represented as $*P < 0.05$, $**P < 0.01$ and $***P < 0.001$. (H, 30 mg/kg/day; L, 15 mg/kg/day; Vin, as vincamine.)

It was found that vincamine effectively improved glucose tolerance (Fig. 9A, B, C and D), but it rendered no effect on ITT (Fig. 9E and F).

In addition, we also examined the effect of vincamine on insulin sensitivity in mouse primary hepatocytes. As shown in Fig. 9G, the insulin signaling cascades (p-IR and p-Akt, (Beale 2013)) responded to insulin stimulation in the rosiglitazone-treated group (an insulin sensitizer (Tiikkainen *et al.* 2004), as a positive control) but not in the vincamine-treated group.

Taken together, the results indicated that vincamine had no influence on insulin sensitivity *in vivo* and *ex vivo*, and further supported that vincamine improved glucose homeostasis via its effect on β-cells.

Discussion

T2DM is a global disease with high morbidity and mortality, and the burden of this disease has not yet been met with the corresponding increase of therapeutic strategies (Vetere *et al.* 2014). The importance of preserving or expanding pancreatic β-cell function or mass has been widely recognized in T2DM treatment. In the current study, we determined that vincamine as a GPR40 agonist efficiently improved glucose homeostasis by ameliorating β-cell dysfunction and promoting GSIS. Additionally, vincamine had no effect on basal insulin secretion *in vivo* (Supplementary Fig. 8A and B), indicative of the potential of vincamine in avoiding fateful hypoglycemic complications (McCall 2012).

https://joe.bioscientifica.com
https://doi.org/10.1530/JOE-18-0432

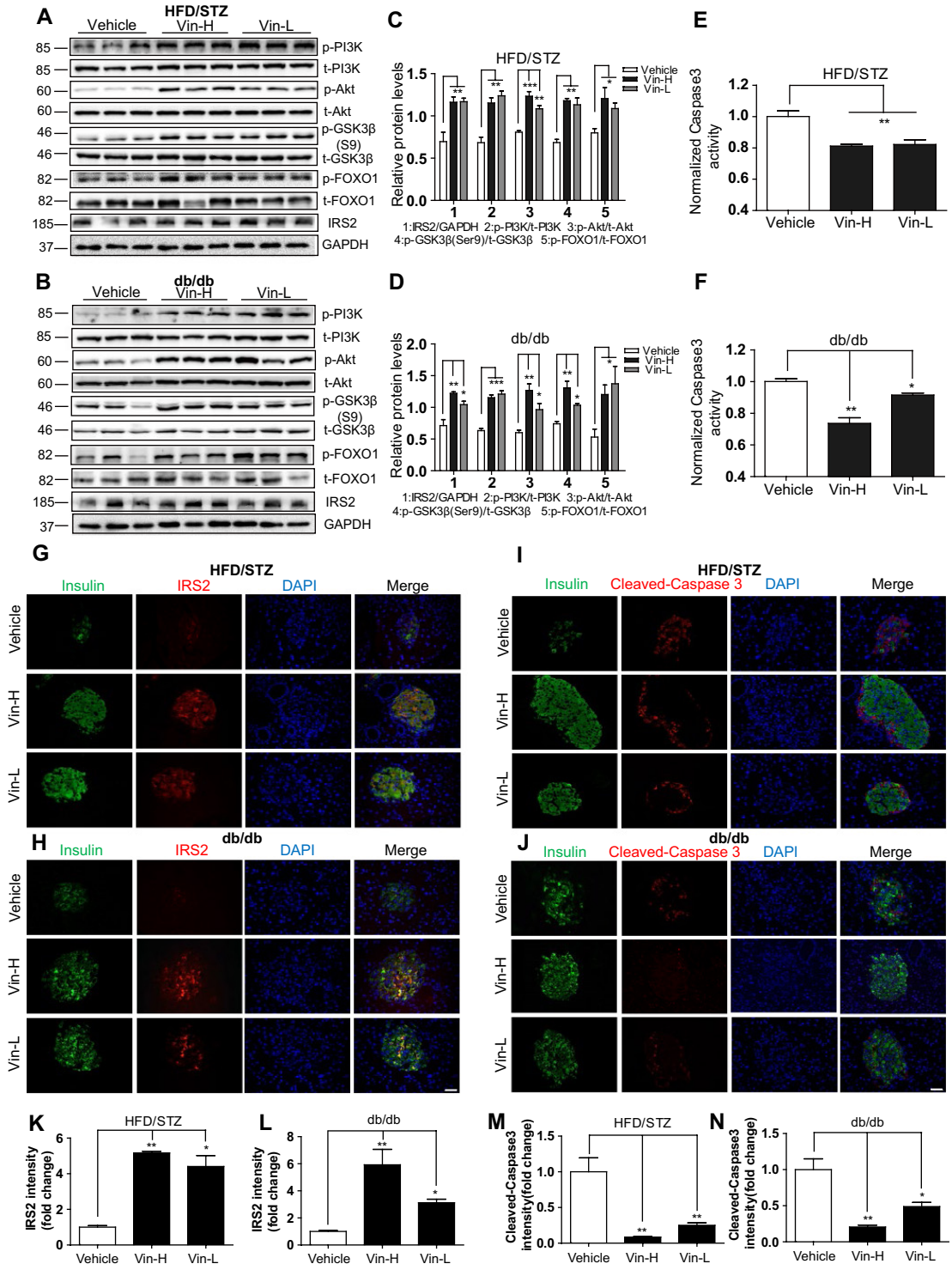

Figure 8

Vincamine modulates IRS2/PI3K/Akt pathway *in vivo*. (A and B) Expressions of the related proteins in IRS2/PI3K/Akt pathway were assayed by Western blot in pancreatic homogenate of HFD/STZ (A) and *db/db* (B) male mice. (C and D) Quantitative results of A and B were displayed correspondingly in C and D. (E and F) Caspase 3 activity in pancreatic homogenate of HFD/STZ (E) or *db/db* (F) male mice was determined by assay kit. (G and H) IF assays for insulin (green) and IRS2 (red) were detected in pancreases of HFD/STZ (G) and *db/db* (H) male mice. (I and J) IF assays for insulin (green) and cleaved Caspase 3 (red) were detected in pancreases of HFD/STZ (I) and *db/db* (J) male mice. The intensity of IRS2 (K and L) and cleaved Caspase 3 (M and N)-positive signals in insulin-positive area was measured. Data were shown as means ± S.E.M. Significant differences between groups are represented as $*P < 0.05$, $**P < 0.01$ and $***P < 0.001$. Bar = 50 μm. (H, 30 mg/kg/day; L, 15 mg/kg/day; Vin, as vincamine.)

https://joe.bioscientifica.com
https://doi.org/10.1530/JOE-18-0432

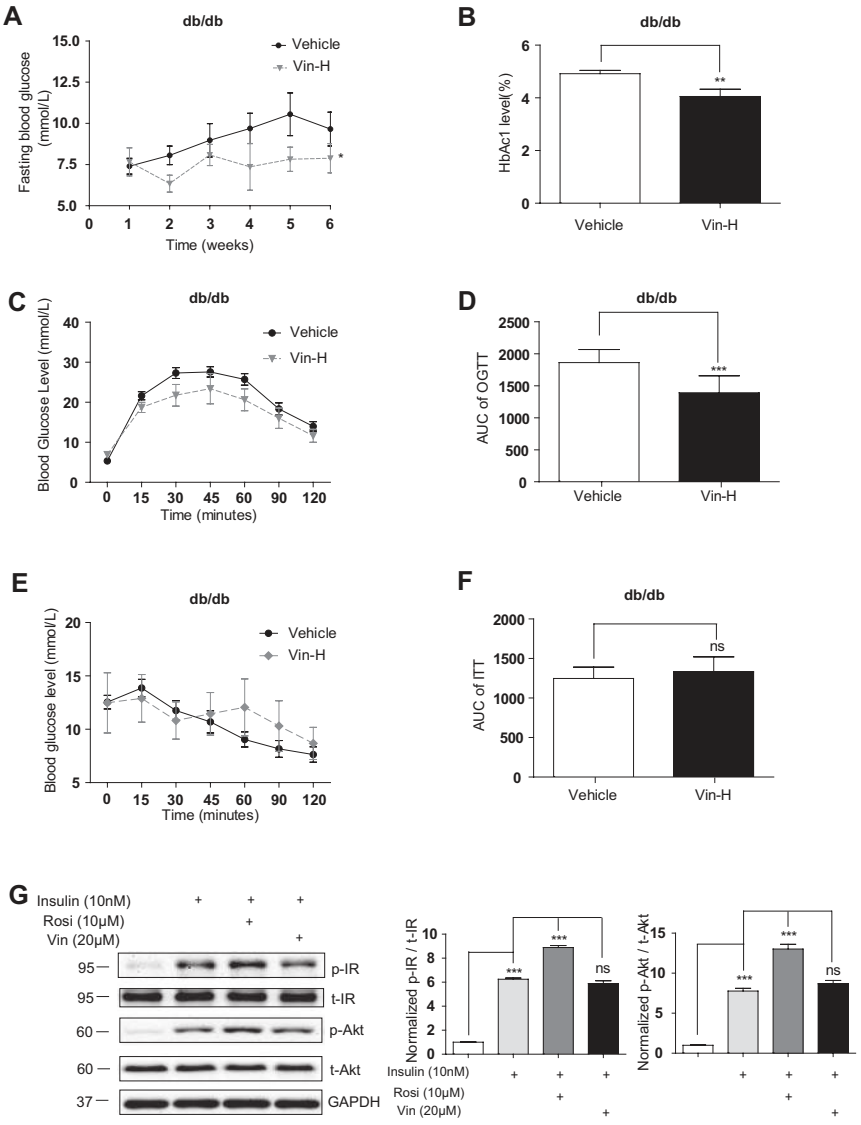

Figure 9

Vincamine has no effect on insulin sensitivity *in vivo* and *ex vivo*. (A) Fasting blood glucose levels of *db/db* female mice were measured weekly. (Black line, vehicle; gray line, 30 mg/kg/day vincamine.) (B) HbA1c levels of *db/db* female mice were detected after vehicle or vincamine (30 mg/kg/day) administration for 6 weeks. (C) Blood glucose levels of *db/db* female mice during i.g. glucose (1.0 g/kg) tolerance tests with vehicle or vincamine (30 mg/kg/day) treatment. (D) was the AUC form of C. (E) Blood glucose levels of *db/db* female mice during i.p. insulin (1.5 U/kg) tolerance tests with vehicle or vincamine (30 mg/kg/day) treatment. (F) was the AUC form of E. (G) Mouse primary hepatocytes were incubated with vincamine (20 μM) or rosiglitazone (10 μM) for 24 h in the presence of insulin (10 nM) for another 15 min, and then the expressions of p-IR and p-Akt were detected by Western blot. Data were shown as means ± S.E.M. with nine mice in each group. Significant differences between groups are represented as $*P < 0.05$, $**P < 0.01$, $***P < 0.001$ and $P > 0.05$ meant no significance (ns). (H, 30 mg/kg/day; Rosi, rosiglitazone; Vin, as vincamine.)

Our findings have thereby highlighted the possibility of vincamine in the treatment of T2DM.

IRS2 is a regulatory adapter protein expressed abundantly in β-cells and acts as an important node linking intracellular and extracellular signals (Oliveira *et al.* 2014). Ablation of IRS2 in whole pancreas caused β-cell mass decrease with reduced β-cell proliferation in the mouse model (Cantley *et al.* 2007). Agents able to upregulate IRS2 may promote β-cell function under physiological stress during T2DM progression (Kuznetsova *et al.* 2016). Currently, our result has clearly demonstrated that vincamine as an upregulator of IRS2 expression *in vivo* and *in vitro* efficiently improved β-cell function, which further supported the key role of IRS2 in β-cells.

GPR40 expresses highly in pancreatic β-cells and mediates free fatty acid in potentiation of insulin, and GPR40 agonist is believed to be promising for anti-T2DM drug discovery (Mancini & Poitout 2015). For example, TAK-875 as a GPR40 agonist has the capacity in lowering blood glucose and entered into Phase III clinical trial, but unfortunately, its further clinical development has to be halted owing to its liver toxicity (Mancini & Poitout 2015). By contrast, vincamine is an approved drug and treated as a natural health care product, showing its safety. Thus, it is believed that vincamine as a new GPR40 agonist should find its application prospect in the treatment of T2DM.

Recently, GPR40 has been mostly reported to promote insulin secretion in β-cells, but there is still controversy that regulation of GPR40 may exert both positive and negative effects on β-cell survival, depending on the concentration and acting duration of GPR40 ligand.

https://joe.bioscientifica.com
https://doi.org/10.1530/JOE-18-0432

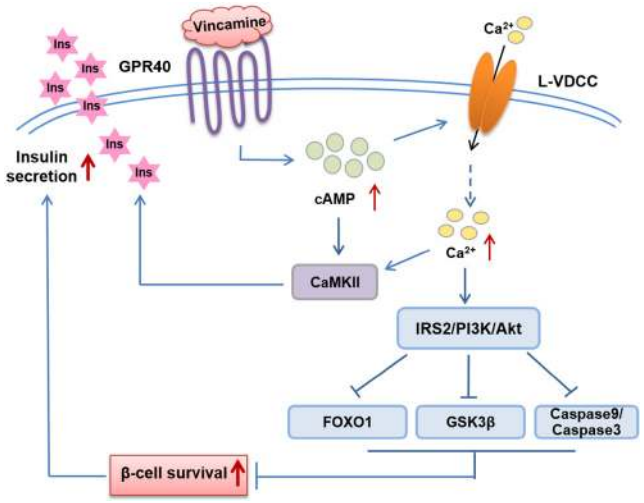

Figure 10
Schematic illustration of the vincamine-mediated β-cell protection and insulin secretion.

Moreover, GPR40 activation may not be associated with pro-apoptotic effect of chronic exposure of FFA, while renders protection against β-cells (Wagner *et al*. 2013). In our work, vincamine activated the downstream anti-apoptotic signaling cascades through GPR40 activation. This scenario is consistent with the report that activation of GPR40 can improve the preservation of pancreatic β-cells through apoptosis inhibition (Gowda *et al*. 2013).

Apart from the capacity in promoting β-cell survival, vincamine also increased β-cell GSIS via GPR40 activation. Currently, the insulinotropic mechanism of GPR40 is only partially understood, in which IP_3 binds to IP_3 receptor (IP_3R) on the endoplasmic reticulum leading to release of Ca^{2+} to promote subsequent insulin secretion (Chen *et al*. 2016). Interestingly, our findings seemed counterintuitive. First, the vincamine-induced promotion of GSIS was un-related to IP_3R activation (Supplementary Fig. 3). Secondly, activation of cAMP and Ca2+/CaMKII was responsible for the vincamine-induced enhancement of GSIS. A tentative explanation is that GPR40 as a Gq-coupled receptor also can signal efficiently through Gs to increase intracellular cAMP (Hauge *et al*. 2015). On the other hand, IP_3 signaling makes little contribution to intracellular Ca^{2+} regulation and insulin secretion in response to FFAs (Mancini & Poitout 2013). In addition, CaMKII activity was essential for vincamine-mediated GSIS, but nifedipine rendered no influence on this effect in accordance with a previous study that CaMKII is an integral Ca^{2+} sensor in a feed-forward pathway that regulates cytosolic Ca^{2+} to enhance insulin secretion (Dadi *et al*. 2014). Therefore, based on the above findings, we tentatively proposed a new mechanism of the GPR40-mediated GSIS using vincamine as a probe.

In conclusion, we reported that vincamine as a GPR40 agonist promoted β-cell protection and GSIS and improved glucose homeostasis in HFD/STZ and *db/db* mice. The mechanisms underlying the anti-T2DM function of vincamine have been fully unraveled, in that vincamine protected against the STZ-induced β-cell apoptosis by regulating GPR40/cAMP/Ca^{2+}/IRS2/PI3K/Akt signaling pathway and promoted GSIS via GPR40/cAMP/Ca^{2+}/CaMKII signaling (Fig. 10). Our findings have highlighted the potential of vincamine in the treatment of T2DM.

Supplementary data
This is linked to the online version of the paper at https://doi.org/10.1530/JOE-18-0432.

Declaration of interest
The authors declare that there is no conflict of interest that could be perceived as prejudicing the impartiality of the research reported.

Funding
This work was supported by the National Natural Science Foundation of China (grant number 81473141 and 81773596), NSFC-TRF collaboration project (grant number NSFC81561148011), Key Laboratory of Receptor Research of the Chinese Academy of Sciences (grant number SIMM1606YZZ-04) and the Priority Academic Program Development of Jiangsu Higher Education Institutions (Integration of Chinese and Western Medicine).

Author contribution statement
Xu shen, Jing Chen and Te Du conceived and designed the study; Te Du carried out the experiments and analyzed the data; Te Du and Liu Yang contributed to interpretation of data; Te Du, Xiaofan Shi, Xin Xu, Xu Xu, Jianlu Lv and Jian Lu performed animal experiments; Lihong Hu contributed the compound in animal experiments; Xu Shen and Te Du wrote the manuscript; all authors, including Heyao Wang and Xi Huang and Jiming Ye discussed the results and approved the final version.

References

Anuradha R, Saraswati M, Kumar KG & Rani SH 2014 Apoptosis of beta cells in diabetes mellitus. *DNA and Cell Biology* **33** 743–748. (https://doi.org/10.1089/dna.2014.2352)

Beale EG 2013 Insulin signaling and insulin resistance. *Journal of Investigative Medicine* **61** 11–14. (https://doi.org/10.2310/JIM.0b013e3182746f95)

Bernal-Mizrachi E, Fatrai S, Johnson JD, Ohsugi M, Otani K, Han Z, Polonsky KS & Permutt MA 2004 Defective insulin secretion and increased susceptibility to experimental diabetes are induced by

reduced Akt activity in pancreatic islet β cells. *Journal of Clinical Investigation* **114** 928–936. (https://doi.org/10.1172/JCI200420016)

Bielefeld-Sevigny M 2009 AlphaLISA immunoassay platform-the 'no-wash' high-throughput alternative to ELISA. *Assay and Drug Development Technologies* **7** 90–92. (https://doi.org/10.1089/adt.2009.9996)

Bonner-Weir S 2000 Life and death of the pancreatic beta cells. *Trends in Endocrinology and Metabolism* **11** 375–378. (https://doi.org/10.1016/S1043-2760(00)00305-2)

Brownlee M 2001 Biochemistry and molecular cell biology of diabetic complications. *Nature* **414** 813–820. (https://doi.org/10.1038/414813a)

Cantley J, Choudhury AI, Asare-Anane H, Selman C, Lingard S, Heffron H, Herrera P, Persaud SJ & Withers DJ 2007 Pancreatic deletion of insulin receptor substrate 2 reduces beta and alpha cell mass and impairs glucose homeostasis in mice. *Diabetologia* **50** 1248–1256. (https://doi.org/10.1007/s00125-007-0637-9)

Chen C, Li H & Long YQ 2016 GPR40 agonists for the treatment of type 2 diabetes mellitus: the biological characteristics and the chemical space. *Bioorganic and Medicinal Chemistry Letters* **26** 5603–5612. (https://doi.org/10.1016/j.bmcl.2016.10.074)

Dadi PK, Vierra NC, Ustione A, Piston DW, Colbran RJ & Jacobson DA 2014 Inhibition of pancreatic beta-Cell Ca2+/calmodulin-dependent protein kinase II reduces glucose-stimulated calcium influx and insulin secretion, impairing glucose tolerance. *Journal of Biological Chemistry* **289** 12435–12445. (https://doi.org/10.1074/jbc.M114.562587)

Dall'Asta M, Bayle M, Neasta J, Scazzina F, Bruni R, Cros G, Del Rio D & Oiry C 2015 Protection of pancreatic β-cell function by dietary polyphenols. *Phytochemistry Reviews* **14** 933–959. (https://doi.org/10.1007/s11101-015-9429-x)

Deeds MC, Anderson JM, Armstrong AS, Gastineau DA, Hiddinga HJ, Jahangir A, Eberhardt NL & Kudva YC 2011 Single dose streptozotocin-induced diabetes: considerations for study design in islet transplantation models. *Laboratory Animals* **45** 131–140. (https://doi.org/10.1258/la.2010.010090)

Elghazi L & Bernal-Mizrachi E 2009 Akt and PTEN: beta-cell mass and pancreas plasticity. *Trends in Endocrinology and Metabolism* **20** 243–251. (https://doi.org/10.1016/j.tem.2009.03.002)

Fandy TE, Abdallah I, Khayat M, Colby DA & Hassan HE 2016 In vitro characterization of transport and metabolism of the alkaloids: vincamine, vinpocetine and eburnamonine. *Cancer Chemotherapy and Pharmacology* **77** 259–267. (https://doi.org/10.1007/s00280-015-2924-3)

Gowda N, Dandu A, Singh J, Biswas S, Raghav V, Lakshmi MN, Shilpa PC, Sunil V, Reddy A, Sadasivuni M, *et al*. 2013 Treatment with CNX-011-67, a novel GPR40 agonist, delays onset and progression of diabetes and improves beta cell preservation and function in male ZDF rats. *BMC Pharmacology and Toxicology* **14** 28. (https://doi.org/10.1186/2050-6511-14-28)

Grimsby J, Sarabu R, Corbett WL, Haynes NE, Bizzarro FT, Coffey JW, Guertin KR, Hilliard DW, Kester RF, Mahaney PE, *et al*. 2003 Allosteric activators of glucokinase: potential role in diabetes therapy. *Science* **301** 370–373. (https://doi.org/10.1126/science.1084073)

Hagstadius S, Gustafson L & Risberg J 1984 The effects of bromvincamine and vincamine on regional cerebral blood-flow and mental functions in patients with multi-infarct dementia. *Psychopharmacology* **83** 321–326. (https://doi.org/10.1007/BF00428538)

Hauge M, Vestmar MA, Husted AS, Ekberg JP, Wright MJ, Di Salvo J, Weinglass AB, Engelstoft MS, Madsen AN, Luckmann M, *et al*. 2015 GPR40 (FFAR1) – combined Gs and Gq signaling in vitro is associated with robust incretin secretagogue action ex vivo and in vivo. *Molecular Metabolism* **4** 3–14. (https://doi.org/10.1016/j.molmet.2014.10.002)

Hofer AM 2012 Interactions between calcium and cAMP signaling. *Current Medicinal Chemistry* **19** 5768–5773. (https://doi.org/10.2174/092986712804143286)

Hosseini A, Shafiee-Nick R & Ghorbani A 2015 Pancreatic beta cell protection/regeneration with phytotherapy. *Brazilian Journal of Pharmaceutical Sciences* **51** 1–16. (https://doi.org/10.1590/S1984-82502015000100001)

Hu H, He LY, Gong Z, Li N, Lu YN, Zhai QW, Liu H, Jiang HL, Zhu WL & Wang HY 2009 A novel class of antagonists for the FFAs receptor GPR40. *Biochemical and Biophysical Research Communications* **390** 557–563. (https://doi.org/10.1016/j.bbrc.2009.10.004)

Huwait EA, Singh NN, Michael DR, Davies TS, Moss JWE & Ramji DP 2015 Protein kinase C is involved in the induction of ATP-binding cassette transporter A1 expression by liver X receptor/retinoid X receptor agonist in human macrophages. *Journal of Cellular Biochemistry* **116** 2032–2038. (https://doi.org/10.1002/jcb.25157)

Ikeda H, Hideshima T, Fulciniti M, Perrone G, Miura N, Yasui H, Okawa Y, Kiziltepe T, Santo L, Vallet S, *et al*. 2010 PI3K/p110 delta is a novel therapeutic target in multiple myeloma. *Blood* **116** 1460–1468. (https://doi.org/10.1182/blood-2009-06-222943)

Ito M, Kondo Y, Nakatani A & Naruse A 1999 New model of progressive non-insulin-dependent diabetes mellitus in mice induced by streptozotocin. *Biological and Pharmaceutical Bulletin* **22** 988–989. (https://doi.org/10.1248/bpb.22.988)

Itoh Y, Kawamata Y, Harada M, Kobayashi M, Fujii R, Fukusumi S, Ogi K, Hosoya M, Tanaka Y, Uejima H, *et al*. 2003 Free fatty acids regulate insulin secretion from pancreatic beta cells through GPR40. *Nature* **422** 173–176. (https://doi.org/10.1038/nature01478)

Jafari R, Almqvist H, Axelsson H, Ignatushchenko M, Lundback T, Nordlund P & Martinez Molina D 2014 The cellular thermal shift assay for evaluating drug target interactions in cells. *Nature Protocols* **9** 2100–2122. (https://doi.org/10.1038/nprot.2014.138)

Kaneko S, Sugimura M, Inoue T & Satoh M 1991 Effects of several cerebroprotective drugs on NMDA channel function: evaluation using Xenopus oocytes and [3H]MK-801 binding. *European Journal of Pharmacology* **207** 119–128. (https://doi.org/10.1016/0922-4106(91)90086-W)

Khorami SAH, Movahedi A, Huzwah K & Mohd Sokhini AM 2015 PI3K/AKT pathway in modulating glucose homeostasis and its alteration in diabetes. *Annals of Medical and Biomedical Sciences*.

Kong X, Yan D, Sun J, Wu X, Mulder H, Hua X & Ma X 2014 Glucagon-like peptide 1 stimulates insulin secretion via inhibiting RhoA/ROCK signaling and disassembling glucotoxicity-induced stress fibers. *Endocrinology* **155** 4676–4685. (https://doi.org/10.1210/en.2014-1314)

Kuznetsova A, Yu Y, Hollister-Lock J, Opare-Addo L, Rozzo A, Sadagurski M, Norquay L, Reed JE, El Khattabi I, Bonner-Weir S, *et al*. 2016 Trimeprazine increases IRS2 in human islets and promotes pancreatic β cell growth and function in mice. *JCI Insight* **1** e80749. (https://doi.org/10.1172/jci.insight.80749)

Leiser M & Fleischer N 1996 cAMP-dependent phosphorylation of the cardiac-type alpha 1 subunit of the voltage-dependent Ca2+ channel in a murine pancreatic beta-cell line. *Diabetes* **45** 1412–1418. (https://doi.org/10.2337/diab.45.10.1412)

Li X, Song D & Leng SX 2015 Link between type 2 diabetes and Alzheimer's disease: from epidemiology to mechanism and treatment. *Clinical Interventions in Aging* **10** 549–560. (https://doi.org/10.2147/CIA.S74042)

Li H, Li Y, Xiang L, Zhang J, Zhu B, Xiang L, Dong J, Liu M & Xiang G 2017 GDF11 attenuates development of type 2 diabetes via improvement of islet beta-cell function and survival. *Diabetes* **66** 1914–1927. (https://doi.org/10.2337/db17-0086)

Mancini AD & Poitout V 2013 The fatty acid receptor FFA1/GPR40 a decade later: how much do we know? *Trends in Endocrinology and Metabolism* **24** 398–407. (https://doi.org/10.1016/j.tem.2013.03.003)

Mancini AD & Poitout V 2015 GPR40 agonists for the treatment of type 2 diabetes: life after 'TAKing' a hit. *Diabetes Obesity and Metabolism* **17** 622–629. (https://doi.org/10.1111/dom.12442)

Markwardt ML, Seckinger KM & Rizzo MA 2016 Regulation of glucokinase by intracellular calcium levels in pancreatic beta cells. *Journal of*

Biological Chemistry **291** 3000–3009. (https://doi.org/10.1074/jbc.M115.692160)

Marquard J, Otter S, Welters A, Stirban A, Fischer A, Eglinger J, Herebian D, Kletke O, Klemen MS, Stozer A, *et al*. 2015 Characterization of pancreatic NMDA receptors as possible drug targets for diabetes treatment. *Nature Medicine* **21** 363–372. (https://doi.org/10.1038/nm.3822)

Mathijs K, Kienhuis AS, Brauers KJ, Jennen DG, Lahoz A, Kleinjans JC & van Delft JH 2009 Assessing the metabolic competence of sandwich-cultured mouse primary hepatocytes. *Drug Metabolism and Disposition* **37** 1305–1311. (https://doi.org/10.1124/dmd.108.025775)

McCall AL 2012 Insulin therapy and hypoglycemia. *Endocrinology and Metabolism Clinics of North America* **41** 57–87. (https://doi.org/10.1016/j.ecl.2012.03.001)

Medarova Z, Bonner-Weir S, Lipes M & Moore A 2005 Imaging beta-cell death with a near-infrared probe. *Diabetes* **54** 1780–1788. (https://doi.org/10.2337/diabetes.54.6.1780)

Molina DM, Jafari R, Ignatushchenko M, Seki T, Larsson EA, Dan C, Sreekumar L, Cao YH & Nordlund P 2013 Monitoring drug target engagement in cells and tissues using the cellular thermal shift assay. *Science* **341** 84–87. (https://doi.org/10.1126/science.1233606)

Moran BM, Flatt PR & McKillop AM 2016 G protein-coupled receptors: signalling and regulation by lipid agonists for improved glucose homoeostasis. *Acta Diabetologica* **53** 177–188. (https://doi.org/10.1007/s00592-015-0826-9)

Oliveira JM, Rebuffat SA, Gasa R & Gomis R 2014 Targeting type 2 diabetes: lessons from a knockout model of insulin receptor substrate 2. *Canadian Journal of Physiology and Pharmacology* **92** 613–620. (https://doi.org/10.1139/cjpp-2014-0114)

Olokoba AB, Obateru OA & Olokoba LB 2012 Type 2 diabetes mellitus: a review of current trends. *Oman Medical Journal* **27** 269–273. (https://doi.org/10.5001/omj.2012.68)

Otters S & Lammert E 2016 Exciting times for pancreatic islets: glutamate signaling in endocrine cells. *Trends in Endocrinology and Metabolism* **27** 177–188. (https://doi.org/10.1016/j.tem.2015.12.004)

Prentki M & Nolan CJ 2006 Islet beta cell failure in type 2 diabetes. *Journal of Clinical Investigation* **116** 1802–1812. (https://doi.org/10.1172/JCI29103)

Reimann F & Gribble FM 2016 G protein-coupled receptors as new therapeutic targets for type 2 diabetes. *Diabetologia* **59** 229–233. (https://doi.org/10.1007/s00125-015-3825-z)

Rodriguez-Diaz R, Dando R, Huang YA, Berggren PO, Roper SD & Caicedo A 2012 Real-time detection of acetylcholine release from the human endocrine pancreas. *Nature Protocols* **7** 1015–1023. (https://doi.org/10.1038/nprot.2012.040)

Saini KS, Thompson C, Winterford CM, Walker NI & Cameron DP 1996 Streptozotocin at low doses induces apoptosis and at high doses causes necrosis in a murine pancreatic beta cell line, INS-1. *Biochemistry and Molecular Biology International* **39** 1229–1236. (https://doi.org/10.1080/15216549600201422)

Shi TJ, Zhang MD, Zeberg H, Nilsson J, Grunler J, Liu SX, Xiang Q, Persson J, Fried KJ, Catrina SB, *et al*. 2013 Coenzyme Q10 prevents peripheral neuropathy and attenuates neuron loss in the db-/db-mouse, a type 2 diabetes model. *PNAS* **110** 690–695. (https://doi.org/10.1073/pnas.1220794110)

Spellman CW 2007 Islet cell dysfunction in progression to diabetes mellitus. *Journal of the American Osteopathic Association* **107** (Supplement) S1–S5.

Srivastava A, Yano J, Hirozane Y, Kefala G, Gruswitz F, Snell G, Lane W, Ivetac A, Aertgeerts K, Nguyen J, *et al*. 2014 High-resolution structure of the human GPR40 receptor bound to allosteric agonist TAK-875. *Nature* **513** 124–127. (https://doi.org/10.1038/nature13494)

Tamura K, Minami K, Kudo M, Iemoto K, Takahashi H & Seino S 2015 Liraglutide improves pancreatic beta cell mass and function in alloxan-induced diabetic mice. *PLoS ONE* **10** e0126003. (https://doi.org/10.1371/journal.pone.0126003)

Tiikkainen M, Hakkinen AM, Korsheninnikova E, Nyman T, Makimattila S & Yki-Jarvinen H 2004 Effects of rosiglitazone and metformin on liver fat content, hepatic insulin resistance, insulin clearance, and gene expression in adipose tissue in patients with type 2 diabetes. *Diabetes* **53** 2169–2176. (https://doi.org/10.2337/diabetes.53.8.2169)

Vetere A, Choudhary A, Burns SM & Wagner BK 2014 Targeting the pancreatic beta-cell to treat diabetes. *Nature Reviews Drug Discovery* **13** 278–289. (https://doi.org/10.1038/nrd4231)

Wagner R, Kaiser G, Gerst F, Christiansen E, Due-Hansen ME, Grundmann M, Machicao F, Peter A, Kostenis E, Ulven T, *et al*. 2013 Reevaluation of fatty acid receptor 1 as a drug target for the stimulation of insulin secretion in humans. *Diabetes* **62** 2106–2111. (https://doi.org/10.2337/db12-1249)

Xu XF, Zhang B, Lu KL, Deng JS, Zhao F, Zhao BQ & Zhao YW 2016 Prevention of hippocampal neuronal damage and cognitive function deficits in vascular dementia by dextromethorphan. *Molecular Neurobiology* **53** 3494–3502. (https://doi.org/10.1007/s12035-016-9786-5)

Yang SN & Berggren PO 2006 The role of voltage-gated calcium channels in pancreatic beta-cell physiology and pathophysiology. *Endocrine Reviews* **27** 621–676. (https://doi.org/10.1210/er.2005-0888)

Zarich SW 2009 Antidiabetic agents and cardiovascular risk in type 2 diabetes. *Nature Reviews Endocrinology* **5** 500–506. (https://doi.org/10.1038/nrendo.2009.150)

Zhao Z, Low YS, Armstrong NA, Ryu JH, Sun SA, Arvanites AC, Hollister-Lock J, Shah NH, Weir GC & Annes JP 2014 Repurposing cAMP-modulating medications to promote beta-cell replication. *Molecular Endocrinology* **28** 1682–1697. (https://doi.org/10.1210/me.2014-1120)

Zheng S, Zhao M, Ren Y, Wu Y & Yang J 2015 Sesamin suppresses STZ induced INS-1 cell apoptosis through inhibition of NF-kappaB activation and regulation of Bcl-2 family protein expression. *European Journal of Pharmacology* **750** 52–58. (https://doi.org/10.1016/j.ejphar.2015.01.031)

Received in final form 15 October 2018
Accepted 2 November 2018
Accepted Preprint published online 2 November 2018